Microfluidic Approach to Control the Macromolecular Concentration and Its Applications in Constructing Phase Diagram of Polymer Aqueous Solution and Screening of Protein Crystallization Conditions

ZHOU, Xuechang

A Thesis Submitted in Partial Fulfillment
of the Requirements for the Degree of
Doctor of Philosophy
in
Chemistry

The Chinese University of Hong Kong
July 2010

Thesis/Assessment Committee

Professor Lam, Sik Lok (Chair)

Professor ZHENG, Bo (Thesis Supervisor)

Professor NGAI, To (Committee Member)

Professor HUANG, Yanyi (External Examiner)

Abstract

This thesis describes a novel microfluidic platform to control the macromolecular concentrations and their applications in constructing the phase diagram of polymer aqueous solutions and in the high-throughput screening of protein crystallization conditions at the nanoliter scale. The microfluidic platform was fabricated using the soft-lithography method and based on poly(dimethylsiloxane) (PDMS) material, which is widely used in microfluidic device. PDMS is gas and water permeable elastomer. By exploiting the permeability of the gas and water in PDMS, we developed the degassed-PDMS nanoliter liquid dispensing system, the controlled microevaporation method in constructing the phase diagram of polymer aqueous solution, and the screening platform of protein crystallization conditions.

This thesis describes two types of degassed-PDMS nanoliter liquid dispensing system. One is dispensing without the microvalve, in which various liquids are dispensed through the degassed PDMS microchannel. It involves two steps: in the first step, the PDMS microchannel patch (or the entire microchip) is placed in a vacuum chamber for a certain time; in the second step, the target liquid is deposited at the inlet of the PDMS channel and dispensed into the PDMS microchamber. The other method is dispensing with the aid of PDMS microvalve. This method combines the valve control and degassed PDMS pumping source, which provides more control over on the liquid dispensing, such as isolating, mixing, etc.

摘要

本論文描述了一種可以控制大分子濃度的新型的微流體平臺,並介紹了它在建立高分子水溶液的相圖和高通量篩選在納升尺度下的蛋白質結晶條件方面上的應用. 這個微流平臺主要是基於一種於微流體系中廣泛應用的PDMS材料.利用到PDMS透氣的性質,我們開發了一種基於脫氣PDMS的納升液體進液系統.利用到PDMS的部分透水性,我們可以進一步控制納升尺度下液體的蒸發,從而實現對填充在納升微井裏面的大分子溶液的濃度控制.

這個基於脫氣PDMS的納升液體進液系統有兩種: 第一種是非閥門控制的液體進液系統.實驗主要分為兩步,首先 PDMS 微流芯片會放入真空中脫氣一定的時間,溶解在PDMS中的空氣濃度會降低.然後,芯片取出來後,放置於常壓下,目標液體樣品就加到微通道的入口,液體就會自動填滿封閉在芯片裏面的所有空間.第二種是帶閥門控制的液體進樣系統.它在第一種系統上加入了閥門的控制,這樣能把真空度暫時儲存在密閉的空間裏面,可以進一步控制液體的進樣,隔離,和混合等.

Acknowledgement

I am very grateful to my supervisor, Professor Bo Zheng. His enthusiasm and kindness, rigorous and honest approach to research, wisdom and rich knowledge of science have left a very deep impression on me. Through the years, he has always encouraged me to work and think independently and efficiently. I learned a lot from him, not only scientific knowledge, but also writing and communicating skills. I would like to thank him for his supervision, guidance and support.

My special thanks go to Professor Chi Wu, for his guidance and discussions on the study of PNIPAM phase diagram using microfluidics.

I would like to thank all the members in Professor Bo Zheng's laboratory for the friendly environment they have created and their helpful discussions. It was very enjoyable working with them.

The financial support of the Chinese University of Hong Kong and the Research Grants Council of Hong Kong is gratefully acknowledged.

Finally, I give my distinguished appreciation to my family for their tremendous support.

Table of contents

Abstract i
摘要 ii
Acknowledgement iii
Table of contents iv
List of tables and figures vi
Chapter 1. Introduction 1
1.1 Introduction to microfluidics 1
1.2 Polymer phase diagram 1
1.3 Protein crystallization 3
1.3.1 Principle of protein crystallization 5
1.3.2 Conventional approaches for protein crystallization 6
1.3.3 Microfluidic approaches for protein crystallization 8
1.4 An outline of this thesis 11
Chapter 2. The degassed PDMS pumping method 13
2.1 Introduction 13
2.2 Experimental 14
2.2.1 The fabrication of SU-8 master 14
2.2.2 The fabrication of PDMS microfluidic device 16
2.2.3 The fabrication of PDMS membrane integrated microfluidic device 16
2.2.4 The fabrication of glass and PMMA microwells 17
2.2.5 The liquid dispensing into microwells without PDMS valve 18
2.2.6 The liquid dispensing with the presence of PDMS valve 20
2.3 Results and discussions 21
2.3.1 The internal vacuum pumping source 21
2.3.2 The efficiency of the pumping 23
2.3.3 The internal vacuum pumping with valve 26
2.4 Conclusion 26
Chapter 3. Constructing the phase diagram of PNIPAM aqueous solution 28
3.1 Introduction 28
3.2 Experimental 28
3.2.1 Design of the microfluidic system 28
3.2.2 Fabrication of the microfluidic device 29
3.2.3 Preparation of the PNIPAM solutions 30
3.2.3 Liquid dispensing, controlled microevaporation and cloud point measurement .. 31
3.3 Results and discussions 33
3.3.1 Controlled microevaporation 33
3.3.2 Cloud points measurements 35
3.3.3 The phase diagram of PNIPAM 36
3.4 Conclusion 37
Chapter 4. High-throughput screening of protein crystallization conditions 39
4.1 Introduction 39

4.2 Experimental 40
4.2.1 Design of the microfluidic system 40
4.2.2 Fabrication of the microfluidic device 42
4.2.3 The procedures of liquid dispensing 43
4.2.4 The procedures of liquid mixing 44
4.2.5 The screening of protein crystallization conditions. 45
4.3 Results and Discussions 45
4.3.1 Screening of protein crystallization conditions 45
4.3.2 The loading of protein and precipitants 46
4.3.2 The mixing of protein and precipitants 48
4.3.3 The concentration control 50
4.4 Conclusion 51
References 53

List of tables and figures

Table 1.1 Important factors affecting macromolecule crystallization.....4

Figure 1.1 The solubility phase diagram for protein crystallization from solution....6

Figure 1.2 The sitting-drop vapor diffusion (left) and microbatch (right) method for protein crystallization.....7

Figure 1.3 The PDMS membrane valve. The image (left) shows the overlap of a control channel and a fluid channel. The image (right) shows the membrane fully deflected into the fluid channel, forming a tight seal. (Image from http://www.fluidigm.com/).....9

Figure 1.4 A schematic illustration of the screening of conditions of protein crystallization by mixing protein solution and precipitants from two microwell patches. Reproduced from reference 56. 11

Figure 1.5 Polarized light micrographs of the protein crystals grown in the microwells with the optimal precipitant. Scale bar: 200 μm. a) Chicken egg-white lysozyme; precipitant: 0.1 M sodium acetate trihydrate buffer, pH 4.6 / 2.0 M sodium formate. b) Horseradish peroxidase; precipitant: 0.2 M $CaCl_2$ / 28% (v/v) PEG 400 / 0.1 M (4-(2-hydroxyethyl)-1-piperazineethanesulfonic acid) (HEPES) buffer, pH 7.5. c) Xylanase; precipitant: 0.2 M $CaCl_2$ / 28% (v/v) PEG 400 / 0.1 M HEPES buffer, pH 7.5. d) Thaumatin; precipitant: 0.8 M potassium sodium tartrate tetrahydrate / 0.1 M HEPES buffer, pH 7.5. Reproduced from reference 56.....11

Table 2.1 Recommended conditions for the SU-8 photoresists.....14

Figure 2.1 A schematic illustration of the UV exposure experimental setup.....15

Figure 2.2 The procedures of the rapid prototyping method to fabricating PDMS microwells.....16

Figure 2.3 The schematic illustration of fabricating the PDMS valve integrated microfluidic device.....17

Figure 2.4 A schematic illustration of the two configurations of liquid dispensing through the degassed PDMS channel patch: a) serial filling using a straight microchannel; b) parallel filling using a branched microchannel. Both of the two configurations have the same three major steps described in the middle column of the figure. 19

Figure 2.5 A schematic illustration of the method of dispensing liquid into an array of microwells through the degassed PDMS microchannel. a) The degassing of the PDMS patch in a vacuum chamber. b) The re-dissolving of air into PDMS from atmosphere. c) The aspiration of the liquid into the microchannel and the microwells after a segment of tubing pre-loaded with the liquid was inserted into the inlet. d) The completion of the dispensing process when the liquid filled up the whole vacancy..21

Figure 2.6 (a) A micrograph of four arrays of circular-shaped microwells filled with aqueous solutions of $Fe(SCN)_x^{3-x}$ (red), $Cu(NH_3)_6^{2+}$ (blue), NaCl (colorless) and $KMnO_4$ (purple), respectively. (b) A micrograph of $Fe(SCN)_x^{3-x}$ aqueous solution in rectangular-shaped microwells with decreasing volume. (c) A micrograph of $Fe(SCN)_x^{3-x}$ aqueous solution in glass microwells. (d) A micrograph of $Fe(SCN)_x^{3-x}$ aqueous solution in PMMA microwells. Scale bar: 2 mm.....22

Figure 2.7 (a) Plot of t_{total} versus t_{degas}. (b) Plot of t_{total} versus $t_{exposure}$. (c) Plot of t_{total} (◆) and $t_{average}$ (◇) versus the number of microwells to be filled via a single PDMS microchannel (n). (d) Plot of t_{total} of different liquids. The error bars were from 5 independent measurements.....24

Figure 2.8 Schematic illustration of the PDMS membrane integrated microfluidic device. 26

Figure 3.1 Schematic illustration of the controlled microevaporation. 29

Figure 3.2 Schematic illustration of the fabrication process of the microfluidic device.....29

Figure 3.3 The assembly of the microfluidic device for constructing the phase diagram.....30

Figure 3.4. Bright-field micrograph of the microchamber filled with an 18.2 wt.-% PNIPAM aqueous solution at 35 °C (above the phase separation temperature), the main channel filled with paraffin oil and the control channel filled with 1.0 M NaCl aqueous solution. 0.5 M $Fe(SCN)_x^{3-x}$ aqueous solution was added into the NaCl solution for better observation.....31

Figure 3.5 Photograph of the experimental setup for cloud point measurement.....32

Figure 3.6. (a) Time dependence of the concentrations of the PNIPAM aqueous solution in the 40 nL microchamber, with the initial concentrations of 18.2 wt.-% (i) and 4.9 wt.-% (ii), respectively. 1.0 M NaCl aqueous solution was flowed in the control channel at the flow rate of 0.5 μL/min; (b) CCD images of PNIPAM aqueous solutions at the indicated concentrations: 18.2 wt.-%, 35.5 wt.-%, and 63.1 wt.-%,

respectively. The white dashed line outlines the microchamber (width 200 μm and length 2 mm) as well as the interface between the PNIPAM solution and the paraffin oil.....34

Figure 3.7. Clouding and clearing curves of the PNIPAM aqueous solution with the concentration of 15.2 wt.-% in the microchamber.....35

Figure 3.8 The multiple times of heating and cooling process. The inlets show the images of the solution at two different temperatures.....36

Figure 3.9. The phase diagram showing the concentration dependence of the phase separation temperatures of PNIPAM aqueous solution. The three curves were from three parallel measurements.....37

Figure 4.1. Schematic illustration of the degassed PDMS microfluidic system with microvalve control for protein crystallization. (a) A basic unit of the design consists of 3 pairs of protein and precipitant microchambers, and 4 reservoirs are filled with the same precipitant. (b) Cross view shows the loading and mixing of solutions... .40

Figure 4.2. The layouts of the designs of the crystallization microchamber layer (a) and the valve layer (b)..... 41

Figure 4.3. Photograph of microfluidic device used for screening of protein crystallization conditions.....42

Figure 4.4. Liquid dispensing process by degassed PDMS and the control of dispensing valves. (a) A red solution was dispensed into the chamber #1 through the degassed PDMS microchannel. (b) The dispensing of the blue solution into the reservoirs, where the blue solution did not enter the chamber #2 due to the dispensing valve was turned off. (c) The dispensing of the blue solution into the chamber #2 by turning on the dispensing valve. (d) The completion of the dispensing, in which the blue solution and red solution did not mix due the mixing valve was maintained off during the entire dispensing process.....43

Figure 4.5. Liquid dispensing and mixing for screening of thaumatin crystallization conditions. (a) 48 precipitants and thaumatin solution were loaded to the inlets. (b) Series of images showing the dispensing and mixing processes. 46

Figure 4.6 The mixing of $Fe(NO_3)_3$ (0.25 M in 15% PEG6K) and KSCN (0.25 M in 15% PEG6K) aqueous solutions controlled by the mixing valve. (a) Loading of aqueous solution into the reaction microchamber, where mixing did not occurred. (b) Time-lapse images showing the mixing process, where the mixing was triggered by the mixing valve. The red color indicated the mixing occurred.....49

Figure 4.7. Polarized light micrograph of the thaumatin crystals grown in the

crystallization microchamber for 20 hours. Thaumatin: 50 mg/ml in 0.1 M N-(2-acetamido)iminodiacetic acid buffer, pH 6.5; precipitant: 0.8 M potassium sodium tartrate tetrahydrate / 0.1 M HEPES buffer, pH 7.5.....51

Chapter 1. Introduction

1.1 Introduction to microfluidics

Microfluidics is the science and technology of systems that process or manipulate small (10^{-9} to 10^{-18} liters) amounts of fluids, using channel with dimensions of tens to hundreds of micrometers.[1] Initially, microfluidics was dedicated to significantly reducing sample consumption and increasing the efficiency of separation.[2-5] Within microfluidics, fluids (liquid or gas) are transported or stored in the microchannel or microchamber for reaction and detection. High resolution and sensitivity of detections and assays are performed with small footprints of the microfluidic devices and small amounts of reagents. As an emerging field, microfluidics is essentially multidisciplinary, including the microfabrication techniques[6,7] and a wide range of applications, such as enzymatic assays,[8] kinetic studies of protein folding,[9] protein crystallization,[10,11] the detection and analysis of DNA.[12-15] Microfluidics not only obtained great successes in analysis, but also found many applications in other fields, such as fluid physics,[16] microbiology[17] and chemical synthesis.[18] etc.

1.2 Polymer phase diagram

Different from small molecules, polymer phase diagrams depend on the chain length. To our knowledge, there is a lack of phase diagrams for most polymers, which is mainly due to two reasons: 1) lack of sufficient amount of narrowly distributed polymer samples with different chain lengths; and 2) an extremely long

time required for a viscous polymer solution to reach its phase equilibrium, especially when the concentration is high. Phase transition of solutions of thermosensitive polymers, such as poly(N-isopropylacrylamide) (PNIPAM), which exhibits a lower critical solution temperature (LCST), has been widely investigated by various experimental techniques, including IR spectroscopy,[19] ^{1}H NMR spectroscopy,[20] viscometry,[21,22] fluorescence,[23] turbidimetry,[24] light scattering,[25] and calorimetry.[26] These studies of the phase transition behavior were generally carried out in conventional reaction vessels with volume of mL or more, and there were two associated issues as aforementioned, i.e., the lack of sufficient amount of narrowly distributed polymer sample and long phase equilibrium time. As a result, systematic experimental investigations on the phase diagram of PNIPAM/water solution have not been accomplished, and the concentration and molecular weight dependence of the cloud point of PNIPAM aqueous solutions are still controversial.[26-30]

Microfluidics platform, with the advantages of small volume consumption, short thermal equilibrium time and high-throughput capability, has been applied to studying the phase behavior and other properties of macromolecules.[31-34] Cremer and coworkers developed a microfluidic device that allowed rapid measurements of the phase separation temperatures of thermosensitive polymer solution stored in glass capillaries.[30,31,35] However, this method required advance preparation of each concentration of the polymer solution to be measured, and it was not feasible for high concentration polymer solution which was too viscous for sample loading. On the other hand, the water permeability of PDMS elastomer[36] has been exploited to

vary the concentration of solutions in the PDMS-based microfluidic device. For example, Leng et al. developed a PDMS microevaporator to concentrate ionic and colloidal solutions,[32] and Lau et al. developed a dynamic osmotic bath for screening conditions of protein crystallization.[33] A "phase chip" was recently designed for studying the phase diagram of various aqueous solutions.[34] These methods demonstrated the feasibility of preparing high concentration with an initial dilute solution by using microfluidic devices. However, all these works utilized multilayer PDMS microfluidic device, which was complicated to fabricate and operate.

1.3 Protein crystallization

Protein crystallization is the bottleneck in determining the tertiary protein structure by X-ray diffraction from sequence data.[37] The completion of the Human Genome Project potentially allows us to identify a host of genetic disorders and design therapies to treat them. However, it is usually not the genes themselves that are the targets but the proteins encoded by them.[38-41] The function of these proteins is determined by their tertiary structures. Therefore, it is essential to get a detailed understanding of the protein structure in order to developing therapeutic treatments and to engineering proteins with improved properties.[41] Many efforts have been spent on it and much progress has been made in the past few years.[42] The most powerful tool to determine 3D protein structure is X-ray crystallography, which requires high-quality protein crystals. Thus, protein crystallization has gained a strategic and commercial relevance in the post-genomic era and there have been

considerable advances in the automation of protein preparation,[43] X-ray analysis,[44] modeling and bioinformatics.[45]

However, protein crystallization is still a rate-limiting step, which has to be achieved by empirical trials and error approaches with hundreds of conditions for each protein.[46] The crystallization of proteins is influenced by a number of factors, which are not independent of each other and their interrelation may be complicated and difficult to distinguish (**Table 1.1**). Therefore, it is difficult to predict which condition can cause the crystallization of a protein. The only way to find the right conditions is to perform a large number of trials to identify these factors individually.

Table 1.1 Important factors affecting macromolecule crystallization.[46]

Physical	Chemical	Biochemical
Temperature/Temperature fluctuation	Buffer pH	Purity of macromolecule
Vibration/Sound/Mechanical perturbation	Precipitant type	Substrates/Coenzyme/Ligand/ Inhibitor/Effectors
Time/Rate of growth	Precipitant concentration	Inherent symmetric of the macromolecule
Equilibrium rate	Macromolecule concentration	Biochemical modification
Dielectric constant of medium	Ionic strength	Genetic/Post-transitional Modification
Viscosity of medium	Additive/Specific ions	Isoelectric point
Pressure	Metal ions	Macromolecule stability
Gravity	Detergent/Surfactant	Aggregation state of macromolecule
Homogeneity of Macromolecule	Degree of supersaturation	Storage time of macromolecule
Electric/Magnetic fields	Reducing/Oxidizing environment	Source of macromolecule
Volume of crystallization sample drop	Present of amorphous substances/impurities	Proteolysis/Hydrolysis
Methodology/Approach of crystallization	Cross-linker	Microbes contamination

In the past several years, there have been some achievements on improving the throughput of protein crystallization screening and lowering the sample consumption by automating and miniaturizing crystallization.[47-49] Thousands of trials are set up per day and the subsequent analysis of the crystallization drops is also progressing at high speed. However, these methods rely on expensive robotic liquid dispensing system and are not widely adopted by individual laboratory. More recently, the PDMS-based microfluidic system provides an alternative to perform protein crystallization at nanoliter scale, with the advantages of lowering the cost, time and reagent consumption.[10,11,33,50,51] However, these methods have some limitations such as complicated background on microfluidics,[10,11] the shortcomings of PDMS materials[52] and the complicated fabrication[7] and operation of the systems.[11] Therefore, developing new crystallization platforms which can be affordable and user-friendly to individual laboratories is still highly desirable.

1.3.1 Principle of protein crystallization

Different from small molecule crystals, protein crystals are labile, fragile and sensitive to the external environment owing to their high solvent content, and the weak binding energies between protein molecules in crystals. The crystallization of proteins from solution is a reversible equilibrium phenomenon. It contains three stages: nucleation, growth and cessation of growth. A classical explanation of crystal nuclei formation and growth can be visualized by the two-dimensional solubility phase diagram (**Figure 1.1**). The solubility curve divides the concentration space into

undersaturated and supersaturated regions. In the undersaturated region, below the solubility curve, the protein will not crystallize. Above the curve, the supersaturated region is subdivided into three regions according to different levels of saturation. In the precipitation region, excess protein exists as an amorphous precipitate, implying no crystals. In the nucleation region, there is a high probability that critical nuclei will form spontaneously in solution. The metastable region is ideal for the growth of crystals without the formation of new crystals. In this region, nuclei will not form, but if nuclei are present or seed crystals are introduced then crystals may grow larger.

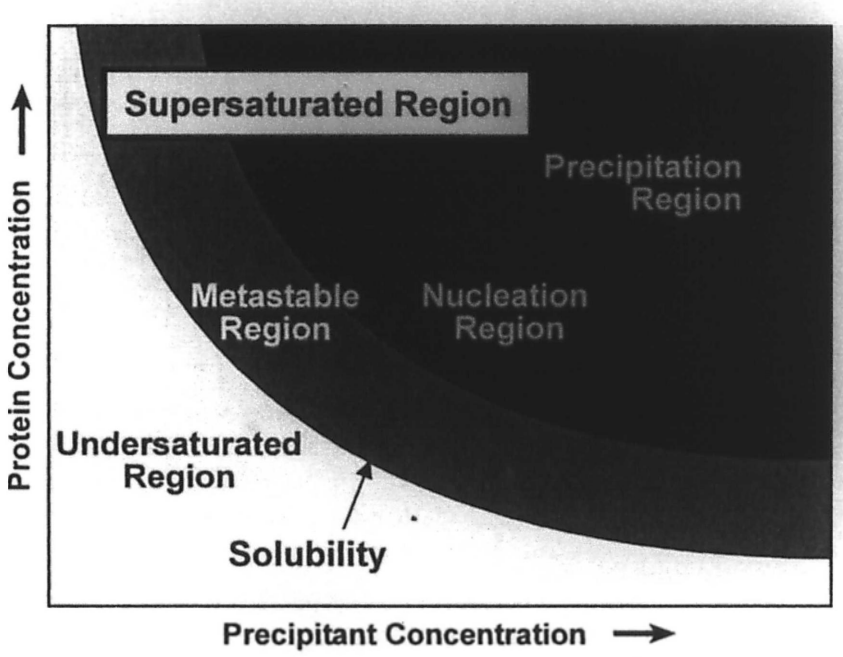

Figure 1.1 The solubility phase diagram for protein crystallization from solution.

1.3.2 Conventional approaches for protein crystallization

There are several techniques for setting up crystallization experiments, including vapor diffusion, batch, microbatch, microdialysis, free interface diffusion and seeding. Among these methods, vapor diffusion and microbatch are the two most common methods which are widely adopted by individual laboratories.[46]

Vapor diffusion is the most widely employed method for protein crystallization. Nucleation occurs when the sample concentration increases as the droplet volume decreases by hydration-driven mechanisms. This is induced by the equilibration of water vapor between the sample droplet and the reservoir solution (**Figure 1.2**). The most common methods of vapor diffusion are the hanging drop and sitting drop. A drop (typically, 1 to 40 μL) containing the protein sample and the crystallization reagent is placed in a sealed chamber, and there is an extra reservoir of crystallization reagent. Thus, the initial reagent concentration is less than that in the reservoir. To reach equilibrium, water leaves the drop and enters the reservoir. During this equilibrium process, the sample is concentrated, increasing the relative supersaturation of the sample in the drop.

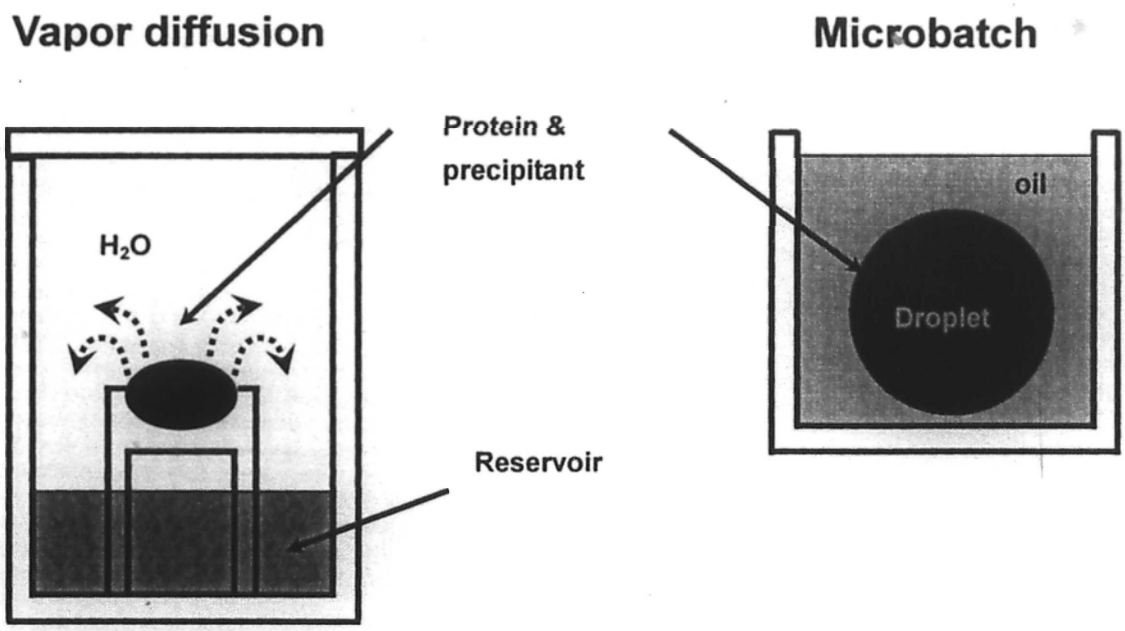

Figure 1.2 The sitting-drop vapor diffusion (left) and microbatch (right) method for protein crystallization.

Microbatch method[53] is another method for rapid protein crystallization using microliters of protein sample per-trial. This method involves direct mixing of the

unsaturated protein solution with precipitating solution, which alters the protein solubility and changes the dielectric properties of the medium to create a supersaturated environment to generate the crystal. In this method, a small drop of the sample (typically, 1 to 2 μL) combined with the crystallization reagent is pipetted under a layer of paraffin oil, which allows little or no evaporation in the drop (Figure 1.2). A modified microbatch can be performed when the drop is placed under a mixture of paraffin oil and silicone oil, or straight silicone oil.[54,55] Such oils allow water vapor to permeate from the drop and concentrate the sample.

1.3.3 Microfluidic approaches for protein crystallization

Since a large number of crystallization experiments are required to uncover the optimal conditions to crystallize a protein, the crystallization of the protein has become challenging, especially when dealing with limited amounts of protein sample. Therefore, developing new strategies with the ability to conduct the protein crystallization in nanoliter volume has attracted much attention and much progress has been achieved in microfluidic systems.

Microfluidics, due to its small dimension of the reaction volume and the unique mass transport properties, which allows the control of molecules in space and time, has become a viable technology for the studies of protein crystallization. Recently, people developed several microfluidic systems for screening of protein crystallization conditions: Free interface diffusion,[10] droplet-based microfluidics,[11,50,51] PhaseChip, [34] microwell-based system,[56] and SlipChip.[57-59]

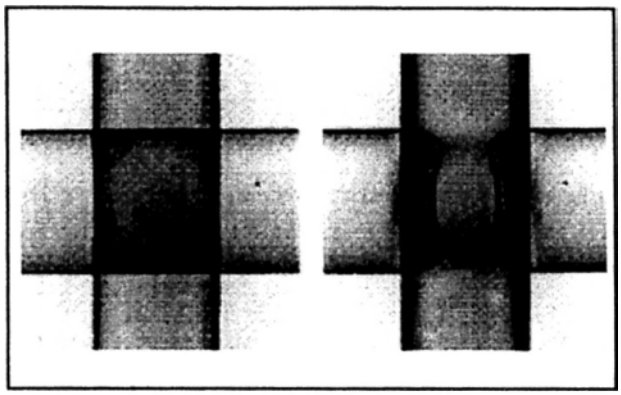

Figure 1.3 The PDMS membrane valve. The image (left) shows the overlap of a control channel and a fluid channel. The image (right) shows the membrane fully deflected into the fluid channel; forming a tight seal. (Image from http://www.fluidigm.com/)

In the free interface diffusion system, the protein solution and precipitants are loaded into microchambers through a large array of valve-controlled identical fluidic units.[10] These pneumatic valves are fabricated of PDMS elastomer using multiplayer soft lithography (MSL) method.[7] The basic microfluidic device was composed of two elastomer layers (**Figure 1.3**). One layer contains channels for flowing liquids (flow layer), and the other layer contains channels that when pressurized with air or nitrogen serve as valves for the flow channels (control layer). When a control channel and a flow channel cross, if the area of the intersection is large enough, a valve is created. The thin membrane separating the two channels deflects into the flow channel when the control channel is pressurized, creating a complete seal. The protein crystallization microchip has 432 active valves and can simultaneously perform 144 crystallization experiments using only 3 μL of protein sample. Conditions of protein crystallization are screened and optimized by free interface diffusion. However, this system has several drawbacks. The 3D fabrication of the pneumatic valves is complicated.[7] In addition, the microchip is made of PDMS

elastomer, which is permeable to many solvents,[52,60] suffering from the lack of long-term storage capability.

The droplet-based microfluidic system allows screening of conditions of protein crystallization in nanoliter size droplets which are generated in the microchannel.[11] In this method, continuous aqueous streams containing the protein and the precipitants are combined and injected into a carrier fluid, forming aqueous plugs/droplets containing the protein and the precipitants. Thousands of droplets are formed in the microchannel, which could flow out and into a glass or Teflon capillary.[50,51] This method has well addressed the issues such as the storage of the crystallizing reagents in glass capillary[50] or Teflon capillary,[51] and the indexing of the concentration in the plugs.[61] Both the microbatch and the vapor diffusion approaches have been successfully preformed in the droplet-based microfluidic system.[50] However, there are still several issues: the size and frequency of the droplets/plugs formation and the spacing of droplets in a continuous flow depend much on the fluid physics, suffering from liquids with different wettabilities and viscosities.[62] In addition, the user interface is not friendly to researchers without background on microfluidics. These issues hinder the adoption of this technique by individual laboratories.

To lower the barrier of the application of microfluidics, we had developed a microwell-based system for screening of protein crystallization (**Figure 1.4** and **1.5**).[56] In this method, screening of protein crystallization conditions was performed by mixing two microwell patches pre-loaded with protein and precipitants by the degassed PDMS microchannel patches.

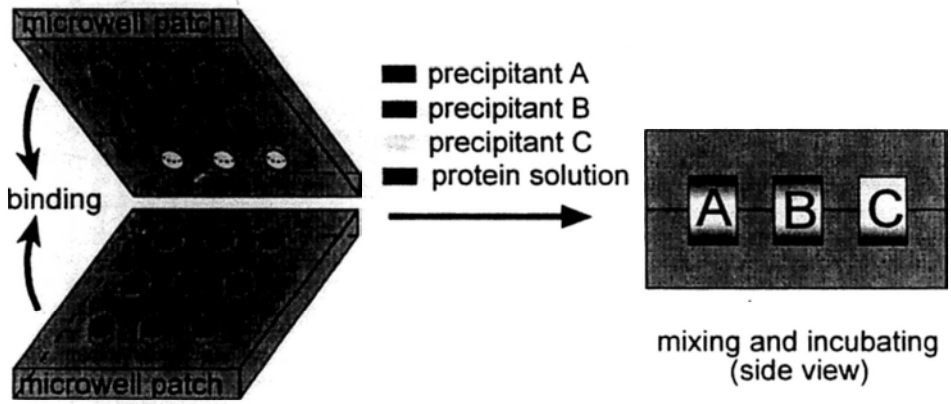

Figure 1.4 A schematic illustration of the screening of conditions of protein crystallization by mixing protein solution and precipitants from two microwell patches. Reproduced from reference 56.

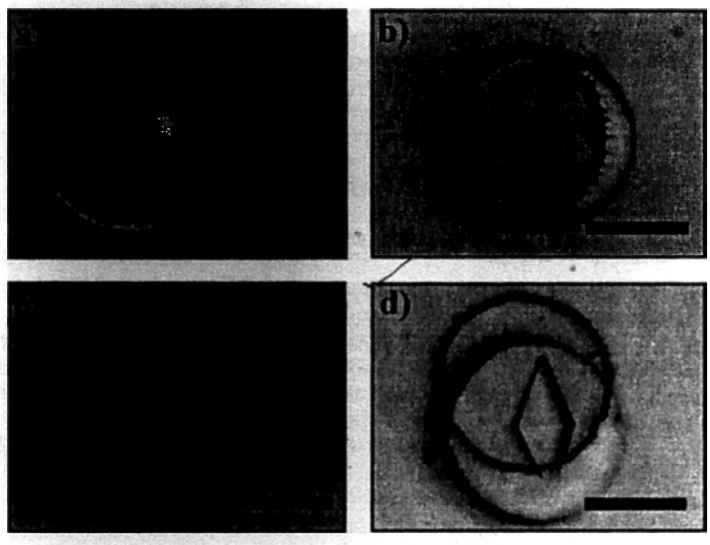

Figure 1.5 Polarized light micrographs of the protein crystals grown in the microwells with the optimal precipitant. Scale bar: 200 μm. a) Chicken egg-white lysozyme; precipitant: 0.1 M sodium acetate trihydrate buffer, pH 4.6 / 2.0 M sodium formate. b) Horseradish peroxidase; precipitant: 0.2 M $CaCl_2$ / 28% (v/v) PEG 400 / 0.1 M (4-(2-hydroxyethyl)-1-piperazineethanesulfonic acid) (HEPES) buffer, pH 7.5. c) Xylanase; precipitant: 0.2 M $CaCl_2$ / 28% (v/v) PEG 400 / 0.1 M HEPES buffer, pH 7.5. d) Thaumatin; precipitant: 0.8 M potassium sodium tartrate tetrahydrate / 0.1 M HEPES buffer, pH 7.5. Reproduced from reference 56.

1.4 An outline of this thesis

This thesis introduces microfluidic approaches for concentration control and their applications in constructing the phase diagram of PNIPAM aqueous solution and high throughput screening of protein crystallization conditions.

Chapter 2 describes a degassed PDMS pumping method for the liquid dispensing

at the nanoliter scale. In this method, PDMS microfluidic device was placed in a vacuum chamber for degassed for a certain time and such degassed PDMS served as an internal vacuum pumping source, by which various liquids were dispensed into the microchannel or microwells. By introducing the PDMS membrane valve into the degassed PDMS pumping system, the internal vacuum pumping power could be temporally stored in the dead-end microchamber, which allowed further controlling the liquid dispensing into the dead-end microchamber.

The construction of phase diagram of PNIPAM aqueous solutions is described in Chapter 3. In this chapter, PNIPAM aqueous solution with defined nanoliter volume was dispensed into a microchamber, where the water molecules permeated from the PNIPAM aqueous solutions to the salt solution with high concentration in the side reservoir microchannel. Phase diagram was obtained by measuring the cloud points of a serial PNIPAM aqueous solution with different concentrations.

Chapter 4 describes a screening platform of protein crystallization condition. This microfluidic platform combined the degassed PDMS pumping methods and PDMS valve system, thus nanoliter of reagents were dispensed into dead-end microchamber through arrays of degassed microchannel and the PDMS dispensing valves. Protein and precipitants were mixed controlled by the mixing valves. One important feature of this system is that individual reservoirs can be filled by their corresponding precipitants during the dispensing process, resulting in a concentration controllable platform for the protein crystallization.

Chapter 2. The degassed PDMS pumping method

2.1 Introduction

The high solubility and permeability of air in PDMS have been exploited in PDMS microfluidic channels to generate flow,[36,63] and to dispense nanoliter liquid into microwells or microchambers.[10,64] Nuzzo and co-workers developed a channel outgas technique,[65,66] in which the inlet of the microfluidic device was immersed in the target solution while the whole system was in vacuum. As the device was brought back to atmosphere, the target solution was infused into the PDMS device due to the reduced pressure in the microchannel. This method consumed at least 20 μL of sample, and was incompatible with solutions containing volatile solvents.[65] Hosokawa *et al.* improved this method by degassing the PDMS device in vacuum and then adding the target solution to the inlet in atmosphere.[63] Hansen *et al.* proposed a method of infusing liquid into nanoliter PDMS chambers by driving the air in the chamber out to atmosphere through PDMS with high external pressure on the liquid.[10] The drawback of this method was the complex fabrication and operation of the PDMS device. These liquid dispensing methods using the permeability of air in PDMS were effective for disposable devices for short-term (hours) analysis, however, long-term (days to weeks) storage, incubation or reactions would be difficult due to the permeability of water and many other solvents in PDMS.[36]

By exploiting the gas permeability of PDMS, we introduced two types of

degassed-PDMS nanoliter liquid dispensing system. In the first various liquids were dispensed through the degassed PDMS microchannel. It involved two steps: in the first step, the PDMS microchannel patch (or the entire microchip) was placed in a vacuum chamber for a certain time, where air concentration depleted; in the second step, the target liquid were deposited at the inlet of the PDMS channel and followed by dispensing into the PDMS microchamber. In the second liquids were dispensed with the aid of PDMS microvalve. This method combined the valve control and degassed PDMS pumping source, which provided more control over on the liquid dispensing, such as isolating, mixing, etc.

2.2 Experimental

2.2.1 The fabrication of SU-8 master

SU-8 master was fabricated using photolithography method.[67] Silicon water (3 inches) was cleaned by immersion in a solution of H_2SO_4/H_2O_2 (v/v 3:1) for 10 minutes. The wafer was rinsed thoroughly with deionized water and dried with compressed air. Then the wafer was further dehydrated in an oven at 110 °C for 1 hour.

Table 2.1 Recommended conditions for the SU-8 photoresists.

Photo resists	Thickness (μm)	Spin speed (rpm)	Soft bake (min)		Post bake (min)	
			t_1(65°C)	t_2(95°C)	t_3(65°C)	t_4(95°C)
SU-8 2100 (*Microchem*)	100	3000	5	20	1	10
	140	2000	5	35	1	15
	260	1000	7	60	1	15
GM 1060 (*Gersteltec*)	10	2555	5	30	5	20
	25	1335	10	35	10	30
	50	565	10	60	10	30

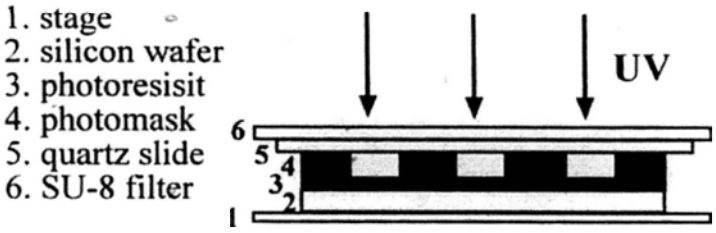

Figure 2.1 A schematic illustration of the UV exposure experimental setup.

Two types of SU-8 photoresist, SU-8 2100 (MicroChem) and GM 1060 (Gersteltec Sarl.), were used to fabricate masters for the microwell and microchannel, respectively. We followed the recommendation parameters of the SU-8 photoresists to fabricate features with different heights (**Table 2.1**). The SU-8 photoresist was poured carefully onto the center of the clean silicon wafer and then coated on the silicon wafer using a spin-coater (KW-4A, IMECAS). The wafer was placed on the 65 °C hotplate and baked for t_1 minutes and further baked at 95 °C for t_2 minutes. Then the wafer was removed and allowed to cool down before UV exposure. A transparency mask was used to pattern the SU-8 photoresist by UV exposure. The experimental setup about the UV exposure step was illustrated in **Figure 2.1**. After the exposure, the wafer was baked at 65 °C hotplate for t_3 minutes and at 95 °C hotplate for t_4 minutes. The wafer was then developed in a bath of SU-8 developer (MicroChem), in which the unexposed photoresist was removed, and then the wafer was rinsed with isopropanol. Finally, the wafer was dried by N_2 flow and stored in the oven at 60 °C before use. Thus, SU-8 masters with different features were fabricated. SU-8 master was treated with "air plasma" (SPI Plasma-Prep II) for 2 minutes and placed in a vacuum desiccator along with several drops of the silanizing agent (tridecafluoro-1, 1, 2, 2-tetrahydrooctyl trichlorosilane) for 2 hours.

2.2.2 The fabrication of PDMS microfluidic device

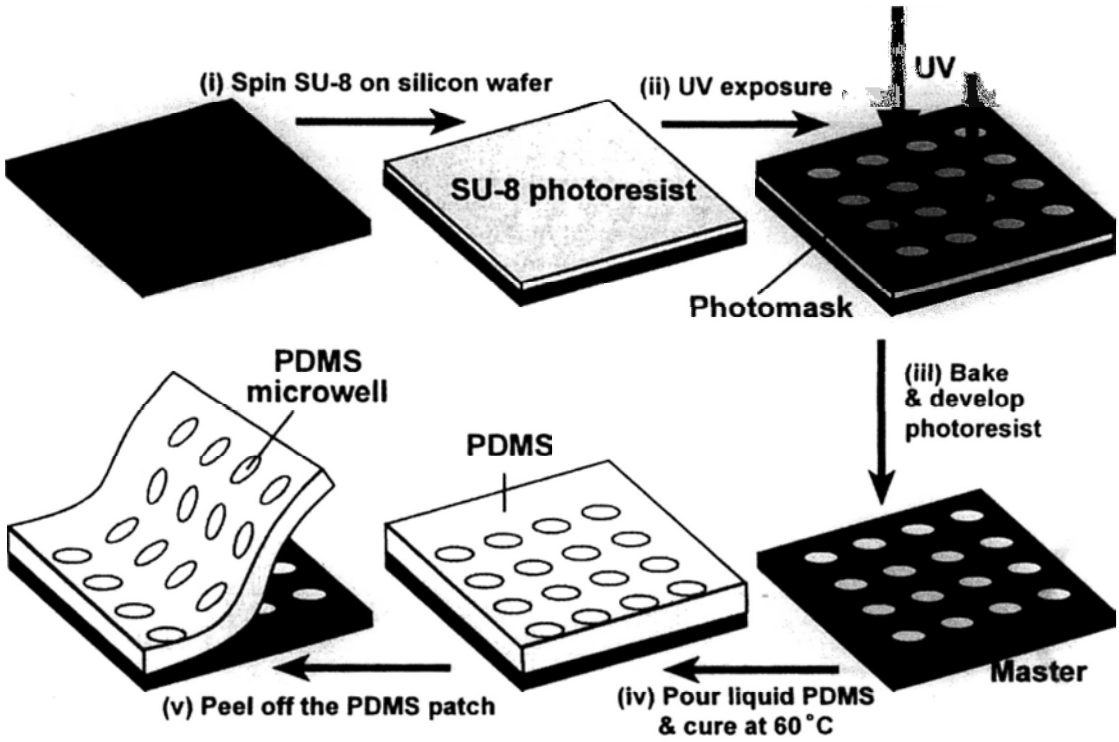

Figure 2.2 The procedures of the rapid prototyping method to fabricating PDMS microwells

PDMS microchannel and microwell patches were fabricated using replica molding method (**Figure 2.2**).[67]

Microchannel and microwell patches with the thickness of 3 mm were then fabricated by casting a 10:1 (in weight) mixture of PDMS precursor and curing agent (Sylgard 184, Dow Corning) against the SU-8 master and curing the mixture at 60 °C for over 2 hours. Finally, the PDMS patches were peeled away from the SU-8 masters.

2.2.3 The fabrication of PDMS membrane integrated microfluidic device

PDMS membrane was fabricated by spin-coated a PDMS precursor (Sylgard 184: curing agent 20:1) on a clean silicon wafer at a speed of 3000 rpm for 60 seconds and then baked at 80 °C for 5 min. The control channel layer was fabricated by baking

the PDMS prepolymer (sylgard 184: curing agent 5:1) at 65 °C for 30 min, followed by peeling apart from the SU-8 master. The control PDMS layer was then bound to the PDMS membrane which was coated on the silicon wafer by baking at 85 °C for half an hour, resulting in a PDMS valve layer. The PDMS valve layer was then reversibly binding to the microwell-patterned PDMS patch, forming the PDMS membrane integrated device (**Figure 2.3**).

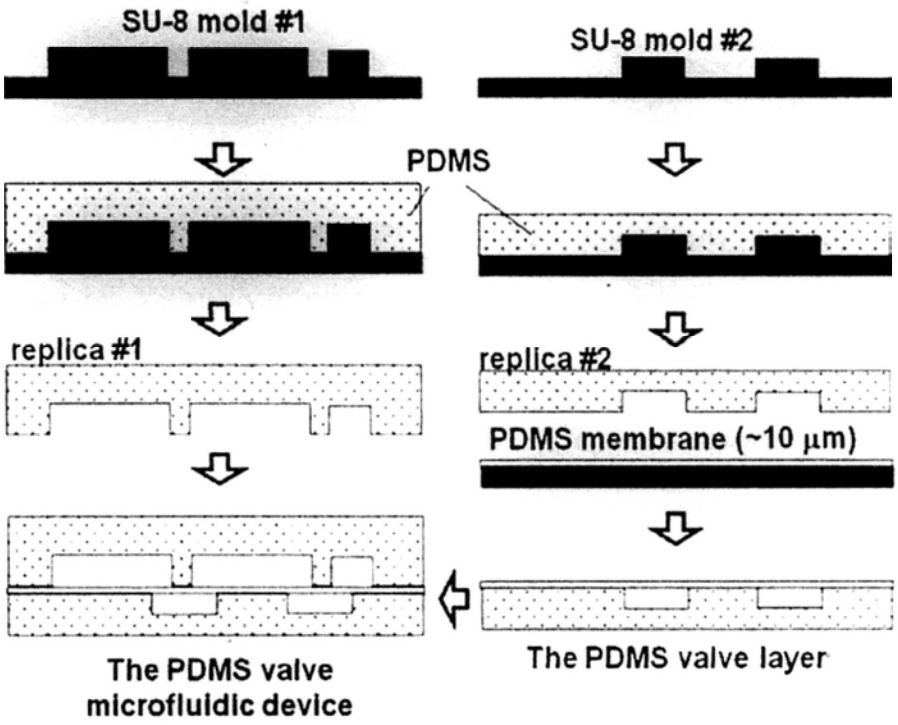

Figure 2.3 The schematic illustration of fabricating the PDMS valve integrated microfluidic device

2.2.4 The fabrication of glass and PMMA microwells

For microwell patches made in glass, glass microscope slides patterned by SU-8 photoresist with the thickness of 100 μm were first fabricated by photolithography. Only the microwell area was exposed. The glass slide was then soaked in 10% HF aqueous solution for 75 minutes, followed by rinsing with deionized water and drying with N_2 flow. The SU-8 photoresist on the microscope slide was removed by

soaking the slide in a solution of H_2SO_4 and H_2O_2 (v/v 3:1) for 10 minutes and then rinsing with deionized water. The depth of the glass microwell was measured by a profilometer (Tencor Alpha-step 500 Surface Profiler) as 110 μm.

Poly(methyl methacrylate) (PMMA) microwells were fabricated by drilling PMMA slides using drill press with a cobalt micro-drill bit with the diameter of 0.30 mm.

2.2.5 The liquid dispensing into microwells without PDMS valve

(a) Assembly of the microfluidic device

A PDMS microchannel patch was reversibly bound with a microwell patch made in PDMS, PMMA or glass, forming a microchip (**Figure 2.4**). Two types of channel-microwell configurations were used in our experiments to introduce liquids into microwells: serial filling and parallel filling. Typically, the dimension of the microchannel was 50 μm in width, and 10 μm in depth. PDMS microwells were 150 μm in depth and glass microwells were 110 μm in depth.

(b) Liquid pre-loading

To prepare Teflon tubing pre-filled with the reagent, a piece of Teflon tubing was attached to a 50 μL syringe. The tubing was then inserted into the reagent. By pulling back the plunger of the syringe, the reagent was aspirated into the tubing at the scale of microliters. Finally the segment of the Teflon tubing containing the reagent was cut off and used for the dispensing. In the control experiment, liquid was directly pipetted at the inlet of the microchannel.

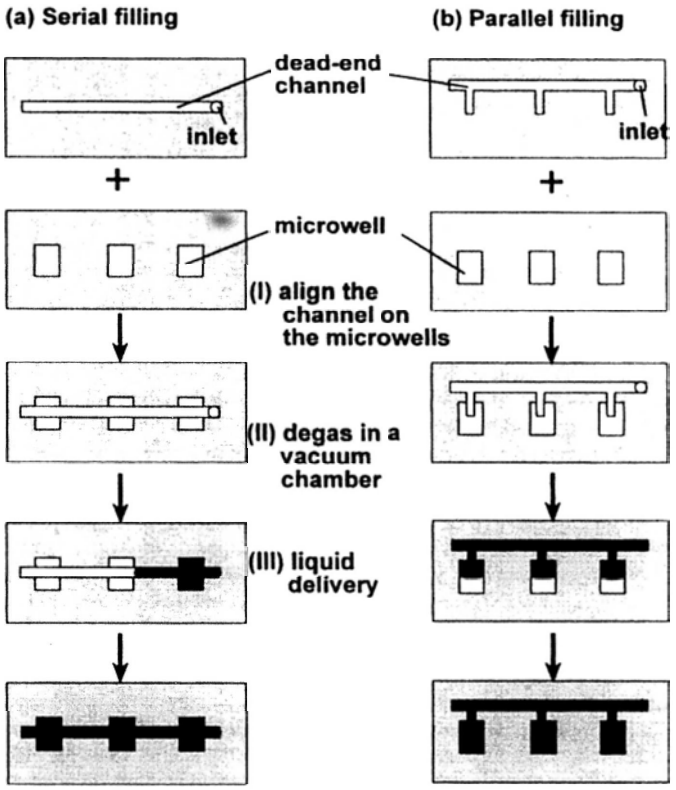

Figure 2.4 A schematic illustration of the two configurations of liquid dispensing through the degassed PDMS channel patch: a) serial filling using a straight microchannel; b) parallel filling using a branched microchannel. Both of the two configurations have the same three major steps described in the middle column of the figure.

(c) Liquid dispensing

Two strategies of the liquid dispensing were present by varying the configuration of the microchannel to achieve serial filling and parallel filling of microwells (**Figure 2.4**).

Serial filling. The microchip was placed in a vacuum desiccator for 30 minutes of degassing at 10 kPa. After the microchip was brought back to atmosphere, a segment of Teflon tubing pre-filled with the reagent was inserted into the inlet of the microchannel to start the dispensing. After the completion of the dispensing process, the microchip was covered with a layer of silicone oil (Fluid 5, Brookfield). The PDMS microchannel patch was then removed from the microwell patch.

Parallel filling. The microchip was placed in a vacuum desiccator for 30 minutes of degassing at 10 kPa. After the microchip was brought back to atmosphere, a segment of Teflon tubing pre-filled with the reagent was inserted into the inlet of the microchannel to start the dispensing. After the completion of the dispensing process, the dead-end of the microchannel was cut off with a sculpture blade. Subsequently, a second liquid, typically, silicone oil or paraffin oil that is immiscible with the aqueous solution was dispensed at the open dead-end. Then the oil was infused into the main channel by pulling backwards the syringe which was previously connected with the inlet of the channel, isolating the reagents in the microwells. Finally the channel patch was peeled off, resulting in arrays of reagents in the microwells. To prevent the evaporation during the storage, paraffin oil was introduced to cover the microwells.

Both the serial filling and parallel filling configurations were used in the experiments. Occasionally some air bubbles formed in the microfluidic channel during the dispensing process, but they disappeared very fast due to the absorption into the degassed PDMS parts, and no clogging was observed during the whole dispensing process. By a combination of serial filling and parallel filling, we managed to increase the throughput of liquid dispensing.

2.2.6 The liquid dispensing with the presence of PDMS valve

The microfluidic was placed in a vacuum desccator for 30 mintues at 10 kPa for degassing. After the microchip was brought back into the atmosphere, liquid was added at the inlet of the microchannel. By pulling back the syringe connected to the

control layer, the valve was turned on. Thus the liquid was dispensed into the dead-end microchamber.

2.3 Results and discussions

2.3.1 The internal vacuum pumping source

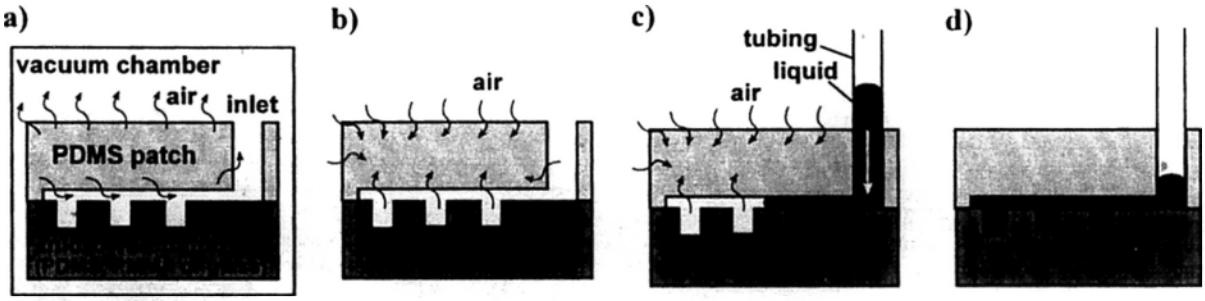

Figure 2.5 A schematic illustration of the method of dispensing liquid into an array of microwells through the degassed PDMS microchannel. a) The degassing of the PDMS patch in a vacuum chamber. b) The re-dissolving of air into PDMS from atmosphere. c) The aspiration of the liquid into the microchannel and the microwells after a segment of tubing pre-loaded with the liquid was inserted into the inlet. d) The completion of the dispensing process when the liquid filled up the whole vacancy.

The mechanism of the degassed PDMS pumping: As shown in Figure 2.5, while the PDMS microchannel patch was placed in a vacuum chamber, the air dissolved in the PDMS was gradually depleted. Once the PDMS patch was taken out and exposed to atmosphere, air slowly diffused back into the PDMS.[63,68] The diffusion occurred both on the surface and through the PDMS microchannel. When the reagent was placed at the inlet to block the air flow into the PDMS microchannel, the internal pressure in the microchannel decreased due to the continuous dissolving of air inside the microchannel into PDMS. As a result, a pressure difference was generated between the internal and external of the microchip. The reagent was aspirated into the microchannel and gradually filled up the whole vacancy of the closed system,

without the formation of air bubbles.

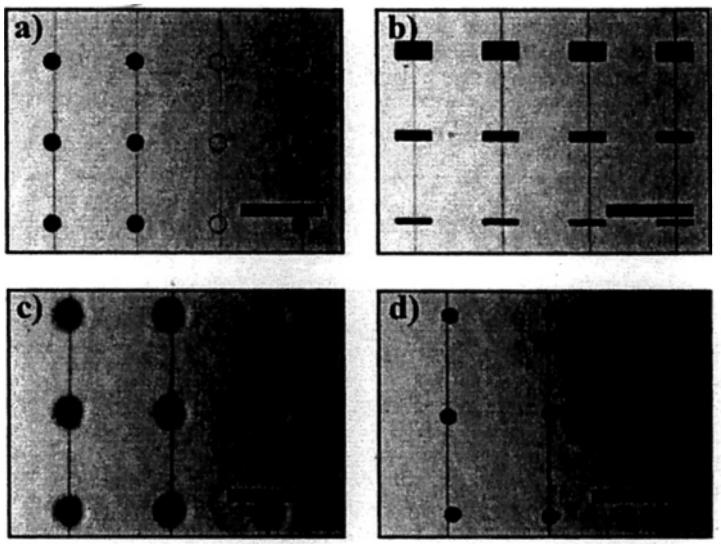

Figure 2.6 (a) A micrograph of four arrays of circular-shaped microwells filled with aqueous solutions of $Fe(SCN)_x^{3-x}$ (red), $Cu(NH_3)_6^{2+}$ (blue), NaCl (colorless) and $KMnO_4$ (purple), respectively. (b) A micrograph of $Fe(SCN)_x^{3-x}$ aqueous solution in rectangular-shaped microwells with decreasing volume. (c) A micrograph of $Fe(SCN)_x^{3-x}$ aqueous solution in glass microwells. (d) A micrograph of $Fe(SCN)_x^{3-x}$ aqueous solution in PMMA microwells. Scale bar: 2 mm.

The dispensing method using degassed PDMS was compatible with microwells of different geometries, sizes and substrate materials **Figure 2.6**). Reagents of different chemical compositions were successfully filled into arrays of microwells by using isolated parallel microchannels (**Figure 2.6a**). The small dimension of the microchannel (50 μm in width and 10 μm in height) facilitated the alignment on top of the microwells of different volumes and geometries (**Figure 2.6b**). The elasticity of PDMS and the negative pressure in the microchannels allowed the PDMS microchannel patch to make conformal contact with many different substrates, and to form leak-free reversible sealing. As a result, microwells fabricated in glass and PMMA were filled smoothly using degassed PDMS microchannels (**Figure 2.6c** and

d).

2.3.2 The efficiency of the pumping

The time needed for filling an array of microwells (t_{total}) is an important parameter for assessing the efficiency of the liquid dispensing. We studied the dependence of t_{total} on four factors: (1) the duration of the degassing process in the vacuum chamber (t_{degas}), (2) the duration when the PDMS microchannel was exposed to atmosphere before the inlet was blocked by the liquid ($t_{exposure}$), (3) the total number of the microwells to be filled through one microchannel (n), and (4) the properties of the liquid, i.e., the viscosity and wettability. In all the experiments, the thickness of the PDMS patches was 3 mm and the dimension of microchannel was 50 μm (width) × 10 μm (height). The microwells were 400 μm in diameter and 150 μm in height, and were fabricated in PDMS. For the first three characterization experiments, water was used as the testing liquid.

Figure 2.7a shows the t_{total} at different t_{degas} for 9 microwells connected by one PDMS microchannel, while the $t_{exposure}$ was constant at 1 minute. The t_{total} decreased rapidly from 9 to 2 minutes as the t_{degas} increased from 1 to 10 minutes. Then the decreasing rate of the t_{total} slowed down significantly, when t_{total} decreased from 2 to 1 minute as the degassing time increased from 10 to 60 minutes. This result indicated the degassing of PDMS patch was reasonably rapid and the air in the PDMS was mostly depleted within the first 10 minutes of the degassing. Therefore, the t_{degas} was set at 10 minutes for the rest experiments.

We then measured the t_{total} at different $t_{exposure}$ for 9 microwells connected by one PDMS microchannel (**Figure 2.7b**). As the $t_{exposure}$ increased, the vacuum level of the PDMS patch decreased, so did the aspiration force for dispensing the liquid. The t_{total} increased almost linearly from 2 to 11 minutes with the $t_{exposure}$ in the range of 1 to 30 minutes. In our experiments, it usually took a few seconds to manually insert one segment of Teflon tubing to start the dispensing, and about 10 minutes to insert fifty segments of Teflon tubing sequentially to dispense fifty different liquids. The very slow decay of the aspiration force of the PDMS patch provided enough time for dispensing such a large number of different liquids. For dispensing liquids of many more than fifty types, a simple automated system that can handle multiple segments of tubing in parallel would be beneficial.

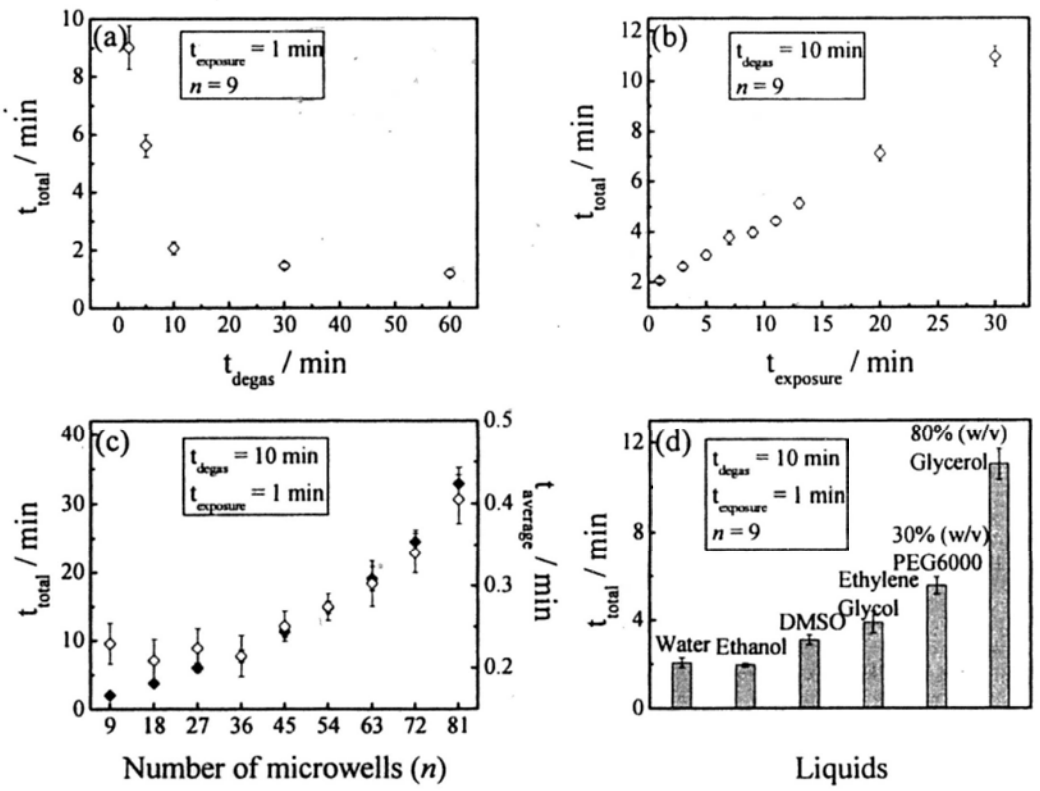

Figure 2.7 (a) Plot of t_{total} versus t_{degas}. (b) Plot of t_{total} versus $t_{exposure}$. (c) Plot of t_{total}

(◆) and $t_{average}$ (◇) versus the number of microwells to be filled via a single PDMS microchannel (n). (d) Plot of t_{total} of different liquids. The error bars were from 5 independent measurements.

We measured the t_{total} versus different total number of microwells (n) to be filled through a single PDMS microchannel, while $t_{exposure}$ was constant at 1 minute (**Figure 2.7c**). The average time for filling each microwell ($t_{average}$) was then calculated as $t_{average} = t_{total} / n$. We found that $t_{average}$ remained constant at about 12 seconds with n ranging from 9 to 36. For larger values of n ($n > 36$), the $t_{average}$ increased almost linearly with n. Therefore, to achieve short average filling time and increase the throughput, parallel microchannels should be employed to fill a large number of microwells.

We also studied the t_{total} of 9 microwells with liquids of different wettabilities and viscosities (**Figure 2.7d**). $t_{exposure}$ was constant at 1 minute. The driving force of the dispensing included the negative pressure in the PDMS microchannel and the capillary force. By comparing the values of t_{total} between the liquids with opposite directions of capillary force and similar viscosity, such as water and ethanol, we concluded that the negative pressure dominated in driving the liquid into the microchannels. Liquids with various viscosities and wettabilities were dispensed reliably through the degassed PDMS microchannels. Among the liquids that we tested, the most difficult type was aqueous solution with high viscosity, e.g., 80% (w/w) glycerol aqueous solution with a viscosity of 44.6 mPa s at 23°C, and the negative pressure was strong enough to aspirate the glycerol solution into 9

microwells in ~ 11 minutes.

2.3.3 The internal vacuum pumping with valve

The integration of PDMS membrane valve into the degassed PDMS liquid dispensing system provides more functions on the liquid dispensing control. As shown in **Figure 2.8**, the microfluidic device consists of a microchamber layer and a PDMS valve layer. The PDMS membrane valve can be turned on/off controlled by a plastic syringe. By pulling the syringe, a vacuum is generated at the control layer, which causes the deformation of the PDMS membrane. Thus, the dead-end microchamber is connected with the fluid. Due to the pre-stored internal vacuum power in the dead-end microchamber generated by the degassed PDMS, the dispensing of the fluid starts again and the dead-end microchamber is completely filled by the fluid.

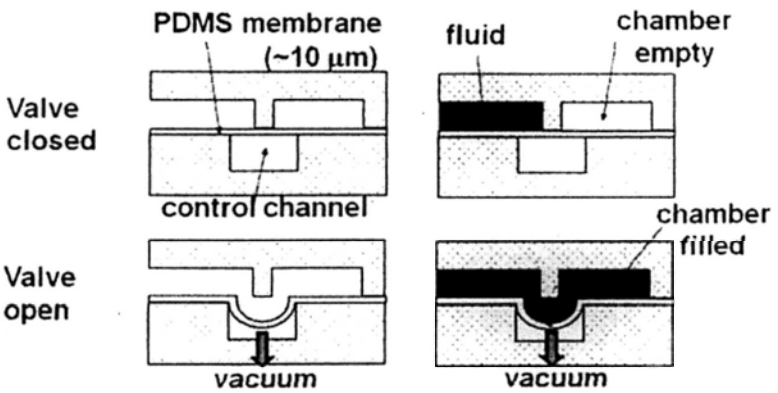

Figure 2.8 Schematic illustration of the PDMS membrane integrated microfluidic device.

2.4 Conclusion

In this chapter, a nanoliter liquid dispensing method is presented to deliver

various reagents into array of microwells through the degassed PDMS channel patch. By exploiting the high gas permeability of PDMS elastomer, a significant vacuum power was generated and stored inside the degassed PDMS patch. When the inlet of the dead-end PDMS channel was blocked by the target liquid, due to the continuous dissolving of air from the sealed chamber into the degassed PDMS parts, a pressure difference was generated and served as a pumping source to start a flow until all the empty space was filled up by the liquid. Moreover, the amounts of the reagents were precisely controlled by employing extremely small filling microchannel. PMMA and glass microwells, and various liquids with different wettabilities and viscosities, were successfully tested by this method. In addition, the integration of PDMS membrane valve into the liquid dispensing system allows the degassed power temporally stored in the dead-end microchamber, which can be restarted by turning on the valve. We envision this degassed PDMS pumping methods may have potential applications in on-chip liquid manipulations, such as the nanoliter liquid dispensing, metering, and mixing.

Chapter 3. Constructing the phase diagram of PNIPAM aqueous solution

3.1 Introduction

In this chapter, we described a single-layer, microchamber-based microfluidic device to study the phase separation behavior of PNIPAM aqueous solution by applying the degassed PDMS liquid dispensing system. By confining the polymer solution in a PDMS microchamber, we were able to concentrate the solution by more than three times and study the phase transition. Comparing to the previous microfluidic devices mentioned above, not only the fabrication and operation are significantly easier, but also the single-layer microchannel facilitates better observation of the phase transition of polymer solutions, e.g., the cloud point.

3.2 Experimental

3.2.1 Design of the microfluidic system

As shown in **Figure 3.1**, the microfluidic system consists of a well defined microchamber which can be loaded with a target solution through a mainchannel. A side microchannel is filled by the high concentration of salt to control the water transportation from the solution confined in the microchamber. As the evaporation goes on, the volume of the solution in the microchamber will decrease. The concentration of the solute in the solution can be calculated by measuring the volume change of the solution in the microchamber.

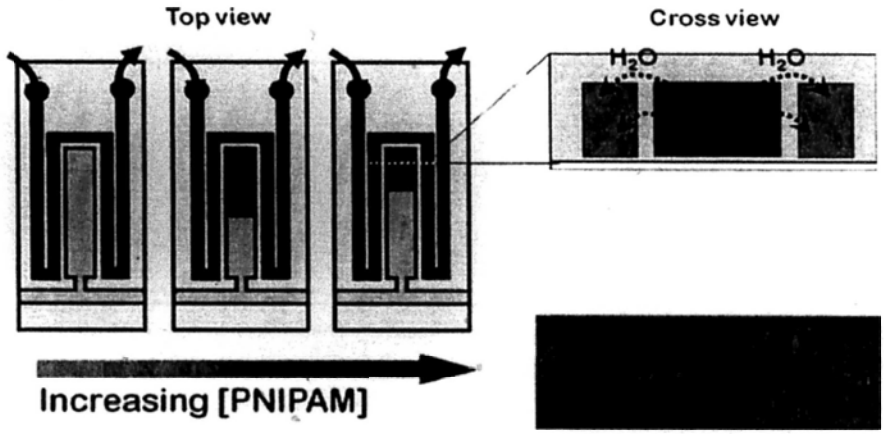

Figure 3.1 Schematic illustration of the controlled microevaporation.

3.2.2 Fabrication of the microfluidic device

The microchip consists of a PDMS patch with patterned features and a PDMS coated glass slide.

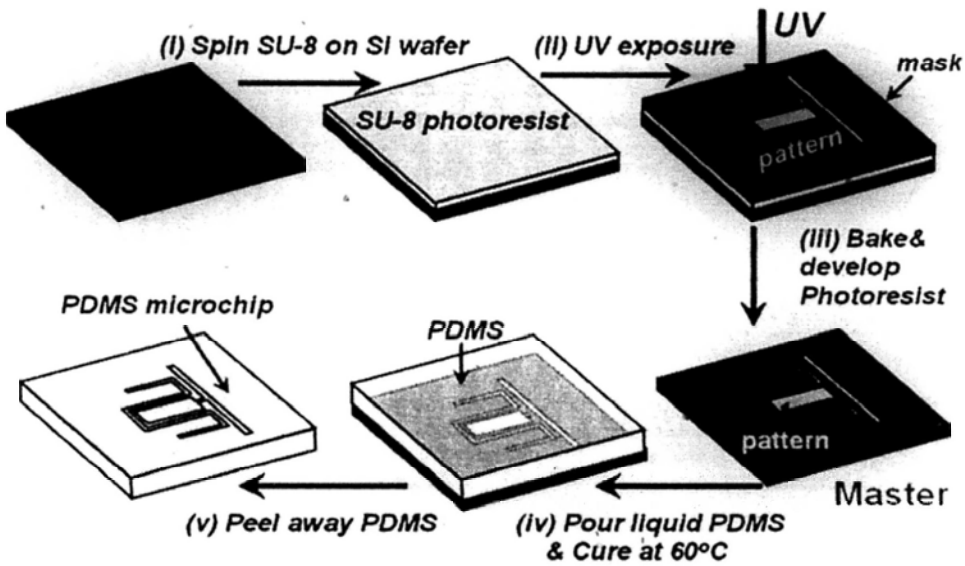

Figure 3.2 Schematic illustration of the fabrication process of the microfluidic device.

The microfluidic device was assembled by irreversibly binding a PDMS slab onto a flat glass slide. As shown in **Figure 3.3**, the glass slide was pre-coated with a thin layer of PDMS. The PDMS slab containing the feature of the microchamber and the microchannels was fabricated by soft lithography (**Figure 3.2**).[67] The microfluidic device contained a microchamber (width 200 μm × length 2000 μm × height 100

μm), a main channel (width 100 μm × height 100 μm), and a control channel (width 100 μm × height 100 μm). The main channel was connected with the microchamber while separated from the control channel.

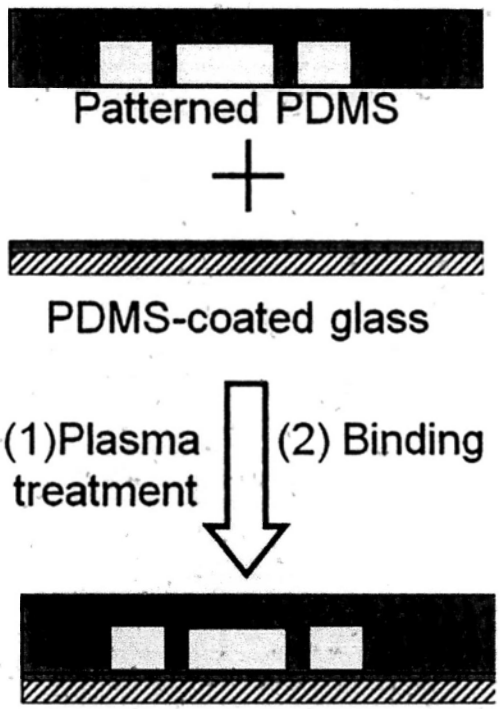

Figure 3.3 The assembly of the microfluidic device for constructing the phase diagram.

3.2.3 Preparation of the PNIPAM solutions

The PNIPAM polymer was synthesized via free radical polymerization [25] and was fractionated using a mixture of acetone/n-hexane at room temperature. The fractionated PNIPAM with a weight-averaged molecular weight (M_w, characterized by laser light scattering) of 3.9×10^5 g/mol and the polydispersity index (PDI, determined by gel permeation chromatography) of 1.10 was chosen for the present study. Two concentrations of the PNIPAM solution in deionized water, 18.2 wt.-% and 4.9 wt.-%, were prepared and used in our experiments.

3.2.3 Liquid dispensing, controlled microevaporation and cloud point measurement

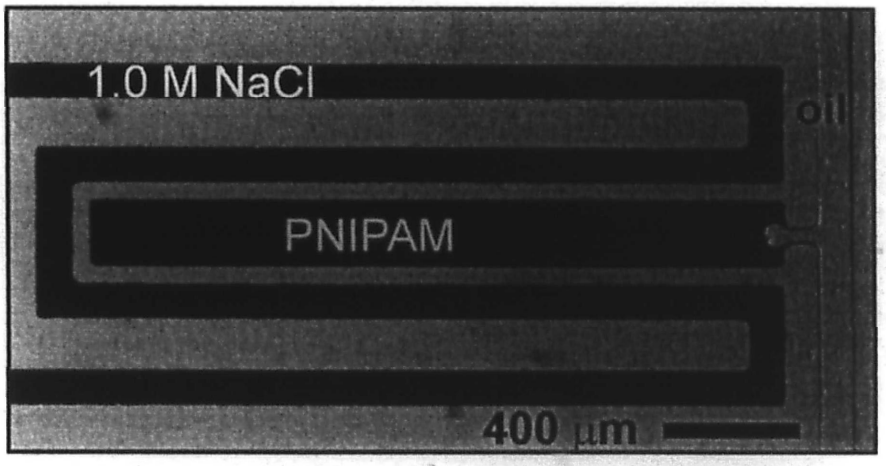

Figure 3.4. Bright-field micrograph of the microchamber filled with an 18.2 wt.-% PNIPAM aqueous solution at 35 °C (above the phase separation temperature), the main channel filled with paraffin oil and the control channel filled with 1.0 M NaCl aqueous solution. 0.5 M $Fe(SCN)_x^{3-x}$ aqueous solution was added into the NaCl solution for better observation.

The PNIPAM aqueous solution was delivered into the microchamber following a previously reported procedure.[56] Briefly, the PDMS device was pre-degassed in a vacuum chamber for 20 minutes. 1 - 2 μL of PNIPAM aqueous solution was preloaded into a segment of Teflon tubing, and the Teflon tubing was inserted into the inlet of the main channel. The outlet of the main channel was also blocked, and vacuum was generated in the main channel and in the microchamber as the air was gradually absorbed into PDMS. As a result, the PNIPAM solution was aspirated into the main channel and the microchamber. After the completion of the filling of PNPAM aqueous solution (18.2 wt.-% or 4.9 wt.-%), paraffin oil was introduced to purge the PNIPAM aqueous solution out of the main channel and confine the PNIPAM solution in the microchamber. To concentrate the PNIPAM solution, 1.0 M

of NaCl aqueous solution was flowed continuously in the control channel at a flow rate of 0.5 μL/min (**Figure 3.4**).

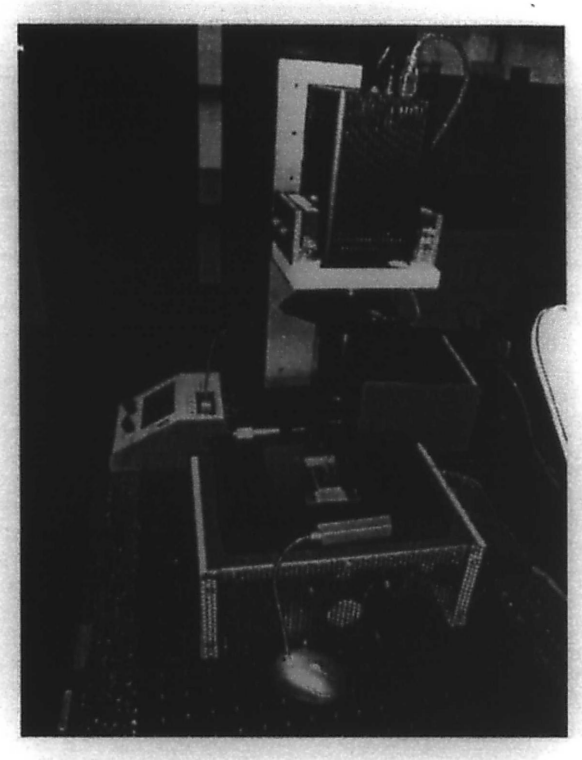

Figure 3.5 Photograph of the experimental setup for cloud point measurement.

Cloud point measurements were carried out when a certain concentration of PNIPAM was reached during the concentrating process. The experimental setup is shown in **Figure 3.5**. The microfluidic device was placed on a programmable Pelt-Plate Intelligent HOT/COLD Plate (Sable Systems International, PELT-5), which was heated or cooled at a rate of 0.5 °C/min. The temperature of the microchannel and the microchamber was recorded by a thermocouple meter (Sable Systems International, TC-2000) which was coupled to the microfluidic device. The phase separation behavior was monitored using a CCD camera (Diagnostic Instruments, SPOT Insight) coupled with a 3× telecentric lens (Daheng) during the heating or cooling process. Series of images were recorded at a speed of 1 frame every 15 seconds. A home-built LED lamp was used as the light source. The

intensity of the scattered light from the PNIPAM solution was measured by ImageJ (NIH). The cloud point was determined as the temperature at which the initial increase of the scattered intensity appeared from the clouding curve during the heating process.[24]We also constructed the clearing curve by measuring the scattered intensity during the cooling process. After the completion of the heating and cooling processes at each concentration, the microfluidic device was cooled down to 15 °C.

3.3 Results and discussions

3.3.1 Controlled microevaporation

A series of PNIPAM aqueous solution with increasing concentration was generated by controlled microevaporation of water in the PDMS microchamber. It has been shown that small neutral molecules such as water can permeate through PDMS relatively easily, [32,33,36,69] while such permeation is non-detectable for ions, such as Na^+ and Cl^-, and for macromolecules such as poly(ethylene glycol) and proteins. [34] In the current microfluidic device, there existed an osmotic pressure difference between the PNIPAM solution and the NaCl solution. Water gradually permeated through PDMS from PNIPAM solution to the NaCl solution, thereby increasing the concentration of PNIPAM. By measuring the volume change of the PNIPAM solution, we were able to determine the concentration of PNIPAM. In addition, the rate of water permeation can be both accelerated and decelerated by using different salt concentrations in the control channel. [34] It is also possible to fine-tune the salt concentration to stop water permeation, [11] so that the polymer

solution will remain at a defined concentration for long-term study.

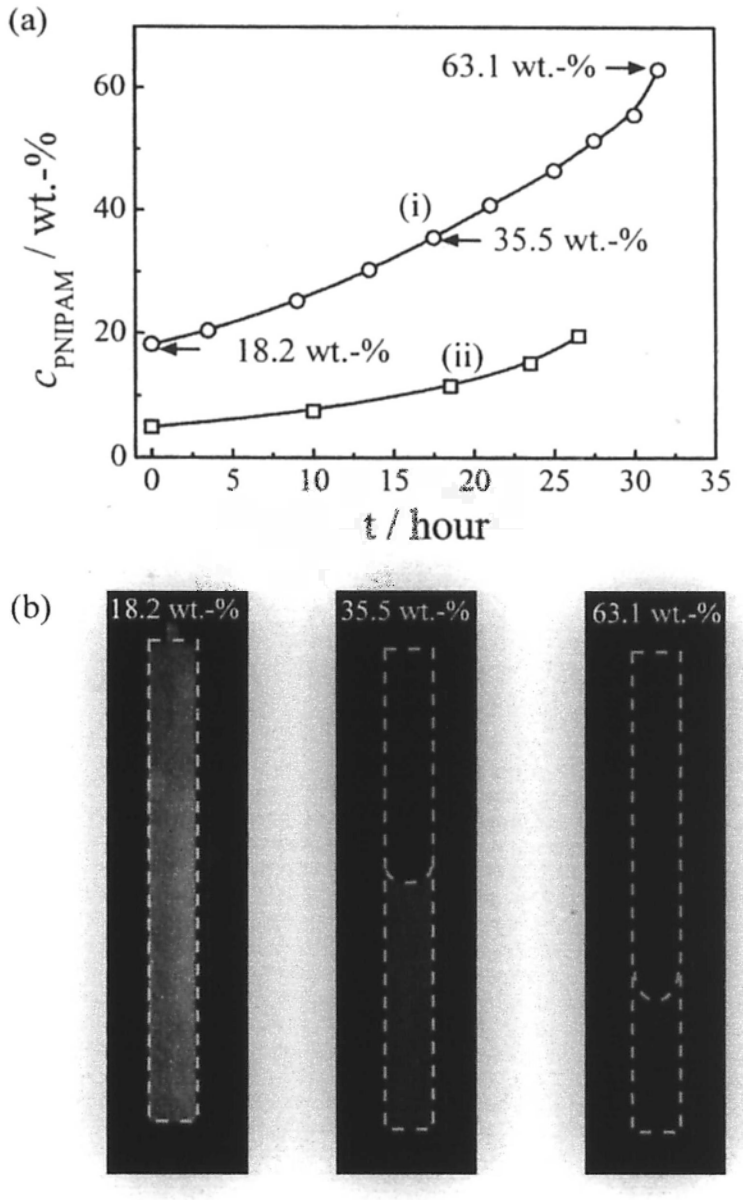

Figure 3.6. (a) Time dependence of the concentrations of the PNIPAM aqueous solution in the 40 nL microchamber, with the initial concentrations of 18.2 wt.-% (i) and 4.9 wt.-% (ii), respectively. 1.0 M NaCl aqueous solution was flowed in the control channel at the flow rate of 0.5 μL/min; (b) CCD images of PNIPAM aqueous solutions at the indicated concentrations: 18.2 wt.-%, 35.5 wt.-%, and 63.1 wt.-%, respectively. The white dashed line outlines the microchamber (width 200 μm and length 2 mm) as well as the interface between the PNIPAM solution and the paraffin oil.

In our experiment, 1.0 M NaCl aqueous solution was continuously flowed in the control channel at a flow rate of 0.5 μL/min, and the change of the concentration of PNIPAM in the microchamber was shown in **Figure 3.6**. With an initial 40 nL

volume of PNIPAM aqueous solution of a given starting concentration (4.9 wt.-% and 18.2 wt.-%, respectively), we were able to generate a series of PNIPAM aqueous solutions *in situ* with increasing concentrations, covering a wide range from 5 wt.-% to 60 wt.-%.

3.3.2 Cloud points measurements

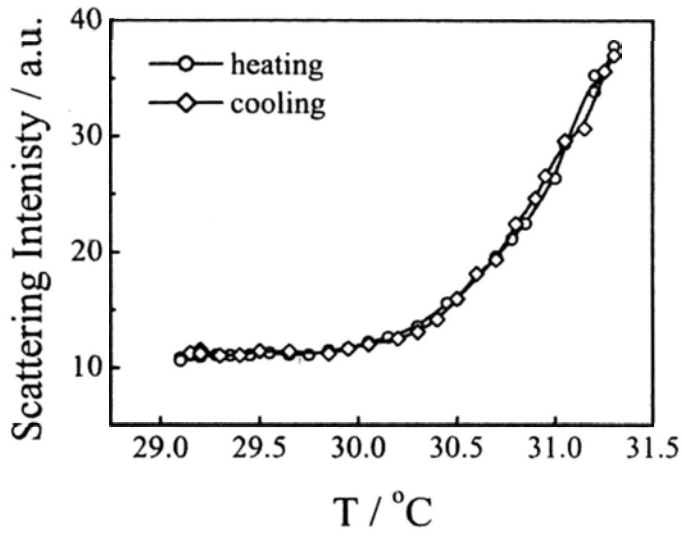

Figure 3.7. Clouding and clearing curves of the PNIPAM aqueous solution with the concentration of 15.2 wt.-% in the microchamber.

As an LCST type polymer, PNIPAM aqueous solution is homogeneous and transparent at temperature lower than LCST, and undergoes a phase separation upon heating beyond the LCST. Such phase separation causes the increase of the scattered light intensity. **Figure 3.7** shows a typical clouding and clearing curves of PNIPAM aqueous solution at the concentration of 15.2 wt.-%. From the clouding curve, the cloud point was determined at 30.0 °C. Due to the small scale of the microchamber (40 nL), thermal equilibrium between the hotplate and the PNIPAM solution was rapidly established at each temperature point. Remarkably, at each measured

concentration we observed that the clouding and clearing curves were well-overlapped, indicating a reversible phase transition of the PNIPAM aqueous solution (**Figure 3.8**). The rapid thermal equilibrium in the microchamber enabled us to obtain the clouding and clearing curves within a short duration of measurement (~10 min). No noticeable change of the solution volume occurred in such a short duration, as indicated by the controlled microevaporation process; therefore, it was a valid assumption that the concentration remained constant during each heating and cooling processes.

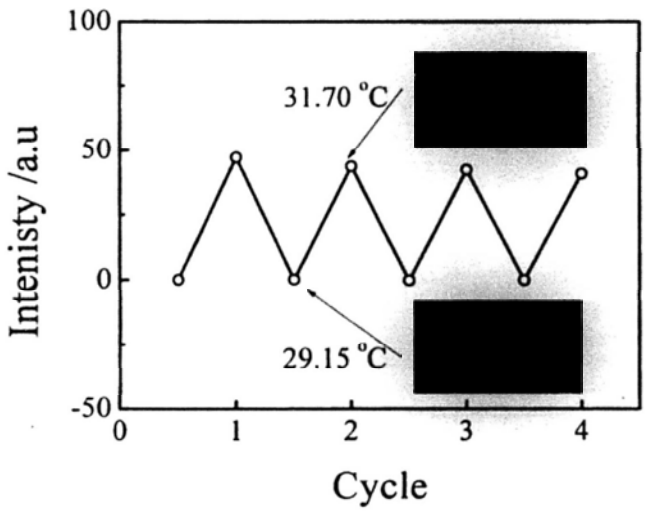

Figure 3.8 The multiple times of heating and cooling process. The inlets show the images of the solution at two different temperatures.

3.3.3 The phase diagram of PNIPAM

The cloud points of a series of concentrations ranging from 5 wt.-% to 60 wt.-% were measured to build the phase diagram of PNIPAM aqueous solution (**Figure 3.9**). Our measurement showed that the phase separation temperatures decreased as the concentration increased in the low concentration region (c_{PNIPAM} < 40 wt.-%)

(**Figure 3.9**). Most of the previous studies about the concentration effect on the phase separation temperature of PNIPAM were limited to the concentration lower than 40 %, [24,30] and our observation showed good agreement. On the other hand, in the high concentration region (c_{PNIPAM} > 40 wt.-%), the phase separation temperature increased as the concentration increased, with a minimum point of the phase separation temperatures at the concentration around 40 wt.-%. This observation was consistent with the results reported by Afroze et al. [70,71] and by Van Durme et al. [29]

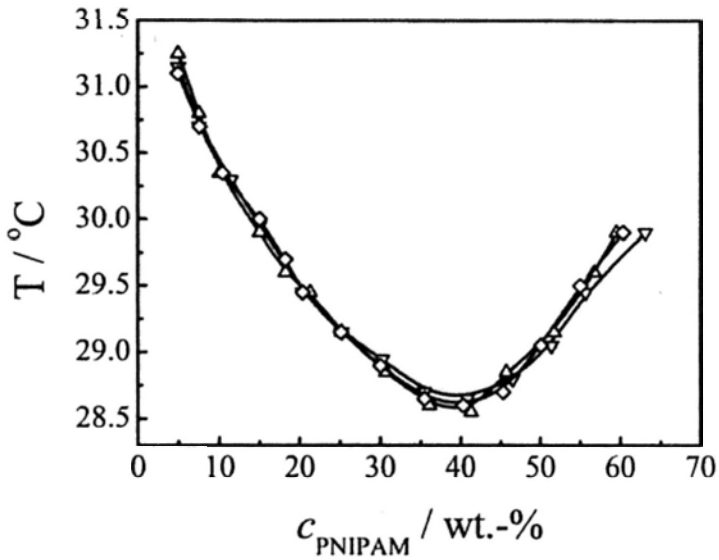

Figure 3.9. The phase diagram showing the concentration dependence of the phase separation temperatures of PNIPAM aqueous solution. The three curves were from three parallel measurements.

3.4 Conclusion

In conclusion, a microfluidic method was developed to construct the phase diagram of PNIPAM aqueous solution. This method has the advantages of simple execution, low sample consumption, rapid heat exchange, and capability of studying high concentration solution. We successfully concentrated the PNIPAM solution to higher than 60 wt.-% by controlled microevaporation, while being still able to

characterize the phase transition in a short duration. The ultrasmall reagent consumption (1 to 2 μL) is important to the study of narrowly distributed polymer sample, which is usually difficult to obtain and the amount is limited. We believe that the microfluidic method is capable of a systematic investigation to ultimately settle the dispute on the effects of concentration and molecular weight on the phase separation temperatures of the PNIPAM aqueous solution. [27,28,30,72] The throughput of the device can be enhanced by improving the following factors: (1) the number of microchambers on the device; (2) the rate of water permeation, which depends on the salt concentration and the PDMS wall thickness between the control channel and the microchamber; (3) the view area of the optical detection setup. Due to the incompatibility of PDMS with many organic solvents,[60] the current PDMS microfluidic device cannot be applied to organic solutions. We envision that this issue can be solved by using fluorinated elastomers as the material of the microfluidic device. [73,74]

Chapter 4. High-throughput screening of protein crystallization conditions

4.1 Introduction

Protein crystallization is a bottleneck in determining tertiary protein structures from the sequence data.[37] The conditions of protein crystallization are usually identified by screening a large number of precipitants under the condition of microbatch or vapor diffusion.[46]

Conventional protein crystallization screening is typically performed by pipetting protein and crystallization reagents together by hand, in which case solutions can be accurately dispensed on the order of 1 μL, or they can be pipetted robotically, in which case solutions can be accurately dispensed on the order of 10 ~ 100 nL. Hand-pipetting is a labor consuming process, while the robotic dispensing systems are expensive and not widely adopted by individual laboratory.

Recently much progress has been achieved in developing microfluidic techniques for protein crystallization with the advantages of little sample consumption and high throughput.[10,11,33,51,75] However, there are still a few issues of protein crystallization in microfluidic devices that impede their adoption in laboratories, including the complex device fabrication and operation,[10,33] and the requirement of sophisticated instrument for flow control.[10,11,51]

Here, we introduced a screening platform of protein crystallization condition as shown in **Figure 4.1**. This microfluidic platform combined the degassed PDMS

pumping methods and PDMS valve system, thus nanoliter of reagents were dispensed into dead-end microchamber through arrays of degassed microchannel and the PDMS valve. Protein and precipitants were mixed controlled by the PDMS mixing valves. One important feature of this system is that individual reservoirs can be filled by their corresponding precipitants during the dispensing process, resulting in a concentration controllable platform for the protein crystallization.

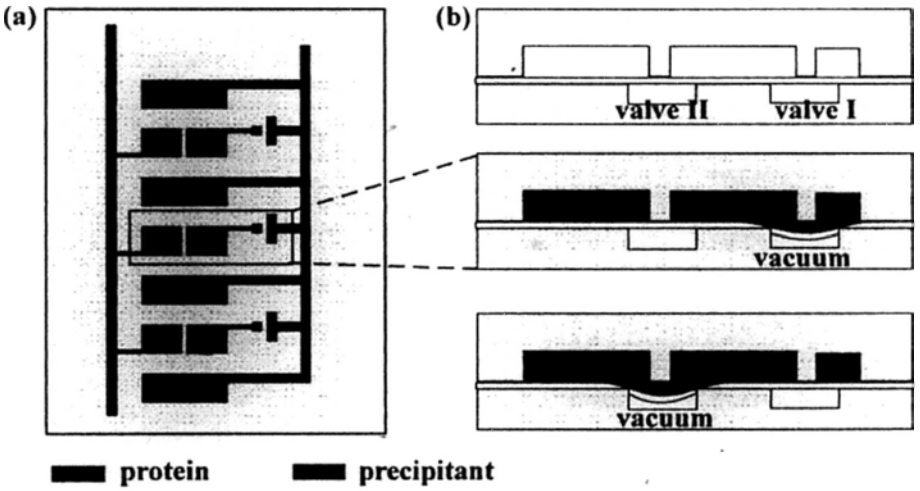

Figure 4.1. Schematic illustration of the degassed PDMS microfluidic system with microvalve control for protein crystallization. (a) A basic unit of the design consists of 3 pairs of protein and precipitant microchambers, and 4 reservoirs are filled with the same precipitant. (b) Cross view shows the loading and mixing of solutions.

4.2 Experimental

4.2.1 Design of the microfluidic system

Crystallization chamber layers with 144 pair of microchambers were fabricated for screening 48 conditions of protein crystallization as shown in **Figure 4.2a**. The purpose was to increase the throughput of the screening up to 144 trials on one microchip and also matched the conventional crystal screening kit (Crystal Screen,

Hampton research).

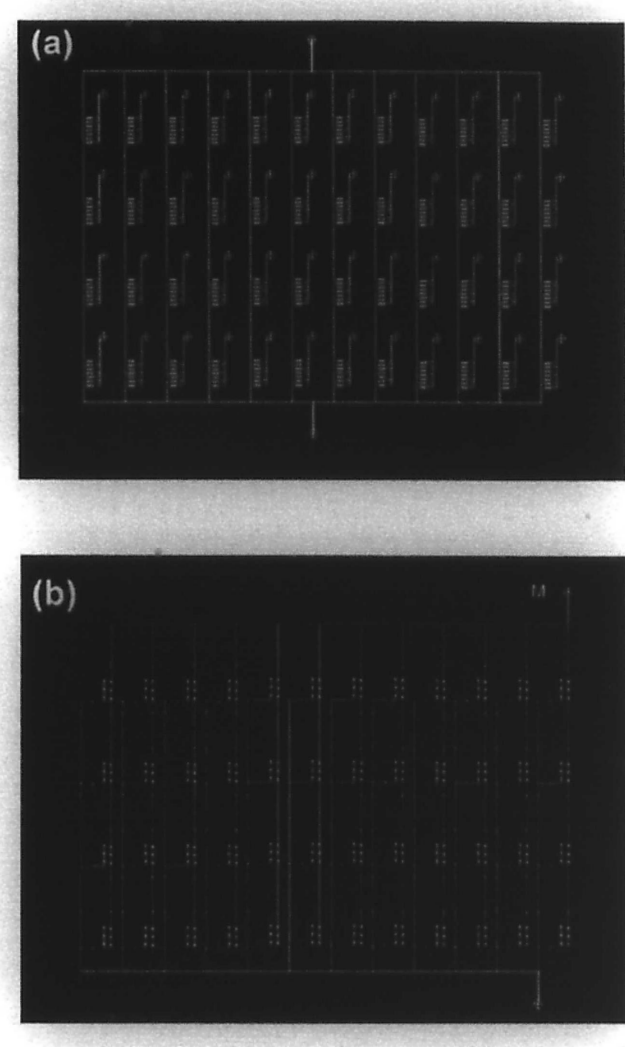

Figure 4.2. The layouts of the designs of the crystallization microchamber layer (a) and the valve layer (b).

Arrays of side microchamber were designed to serve as side reservoirs as shown in the magnified image in **Figure 4.1**. The side reservoir chamber and the precipitant microchamber were not connected. A valve layer consisted of two types of valve, the dispensing valve and the mixing valve (**Figure 4.1**). Valve I was designed to control dispensing of precipitants into the precipitant microchamber and also to isolate the solutions stored in precipitant and reservoir microchamber. The valve II served as the mixing valve. The precipitant and protein microchamber was connected when turning on the valve II. There were two inlets for these two types of valves. And the valves can be controlled through two plastic syringes. In the current design, by

controlling the plastic syringe, 144 precipitant microchambers will be dispensed with precipitants simultaneously and also the mixing of 144 pairs of microchamber.

4.2.2 Fabrication of the microfluidic device

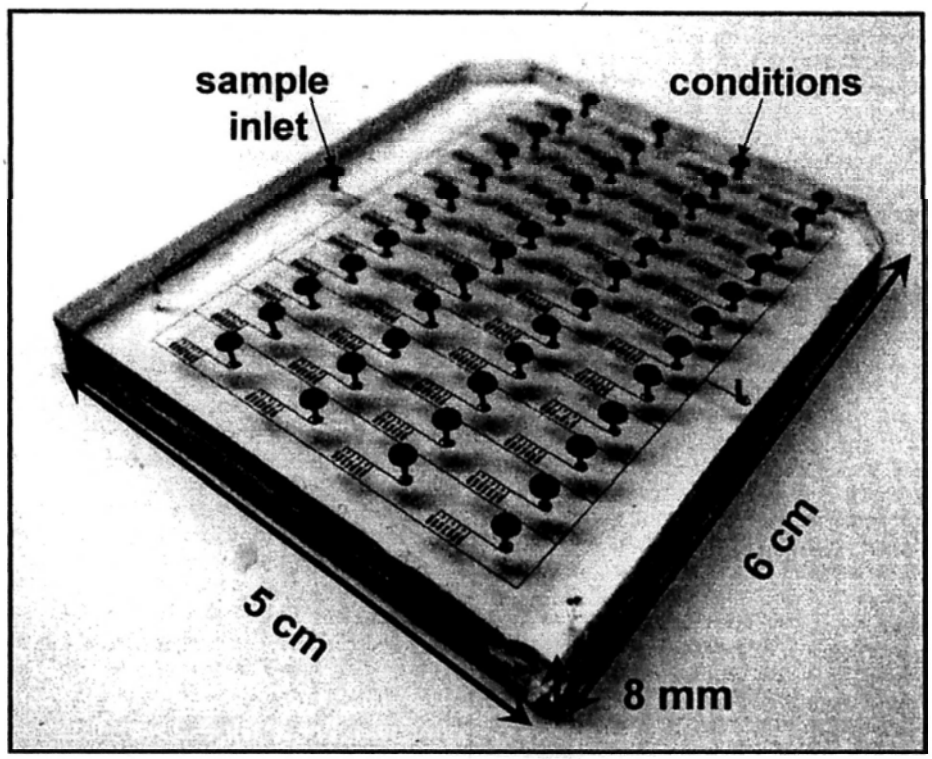

Figure 4.3. Photograph of microfluidic device used for screening of protein crystallization conditions.

The device was fabricated as described in Chapter 2. PDMS membrane was fabricated by spin-coated a PDMS precursor (Sylgard 184: curing agent 20:1) on a clean silicon wafer at a speed of 3000rpm for 60 seconds. And then baked at 80 °C for 5 min. The control channel layer was fabricated by baking the PDMS prepolymer (sylgard 184: curing agent 5:1) at 65 °C for 30 min, followed by peeling apart from the SU-8 master. The control PDMS layer was then bound to the PDMS membrane which was coated on the silicon wafer by baking at 85 °C for half an hour, resulting in a PDMS valve layer. The PDMS valve layer was then reversibly binding to the

microwell-patterned PDMS patch, forming the PDMS membrane integrated device.

Figure 4.3 shows a PDMS microchip filled by the blue and red dye solutions.

4.2.3 The procedures of liquid dispensing

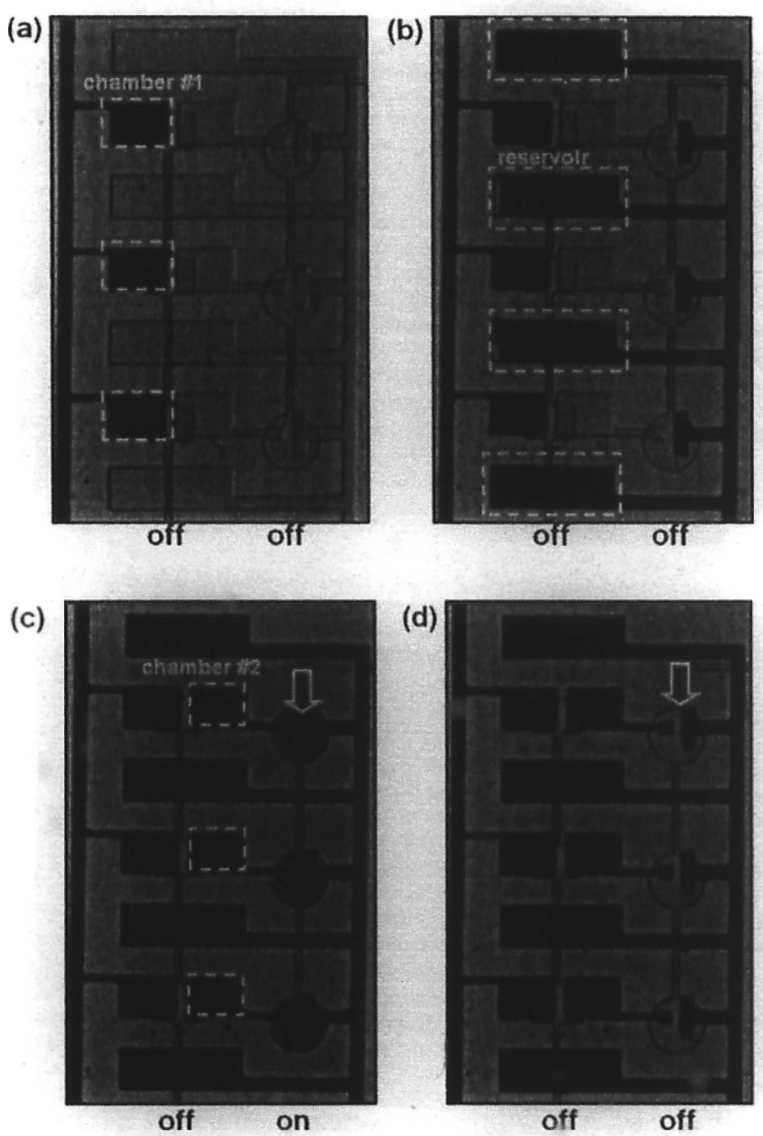

Figure 4.4. Liquid dispensing process by degassed PDMS and the control of dispensing valves. (a) A red solution was dispensed into the chamber #1 through the degassed PDMS microchannel. (b) The dispensing of the blue solution into the reservoirs, where the blue solution did not enter the chamber #2 due to the dispensing valve was turned off. (c) The dispensing of the blue solution into the chamber #2 by turning on the dispensing valve. (d) The completion of the dispensing, in which the blue solution and red solution did not mix due the mixing valve was maintained off during the entire dispensing process.

Figure 4.4 shows the process of the liquid dispensing. Briefly, the device was placed in a vacuum chamber (10kPa) for 30 min and then the device was brought back to atmosphere. For demonstration, a red dye solution was added at the inlets for the microchannel connected to the protein microchamber and then the solution was dispensed into the protein microchamber. A blue dye solution was then added at the inlet of the microchannel for the reservoir and then the reservoir was filled by the blue solution. Afterwards, the dispensing valve was turned on by the pulling the plastic syringe and blue solution was then dispensed into the precipitant microchamber. After the completion of the precipitant microchamber, the dispensing valve was turned off, isolating the solutions from the precipitant and reservoir microchambers.

4.2.4 The procedures of liquid mixing

The mixing of solutions from the protein microchamber and precipitant microchamber was demonstrated by the mixing $Fe(NO_3)_3$ and KSCN aqueous solutions. In the experiment, using the dispensing procedures as described above, $Fe(NO_3)_3$ (0.25 M in 15% PEG6K) and KSCN (0.25 M in 15% PEG6K) aqueous solutions were dispensed into the protein and precipitant microchamber, respectively. And then paraffin oil was introduced to isolate the protein microchamber. Afterwards, the mixing valve was turned on by pulling the plastic syringe, resulting in the mixing of solutions from the protein and precipitant microchamber.

4.2.5 The screening of protein crystallization conditions.

This microfluidic platform was tested by the screening of thaumatin crystallization conditions. The platform contained 144 pair of reaction microchambers, in which 48 conditions was screened. Using the dispensing process as described above, a solution of thaumatin (Wako, Japan) (50 mg/ml in 0.1 M N-(2-acetamido)iminodiacetic acid buffer, pH 6.5) and 48 precipitants from the commercial crystal screening kit (Crystal Screen, Hampton research) were used to dispense into the protein and precipitant microchamber, respectively. The side reservoir microchambers were also dispensed by the corresponding precipitants. After the dispensing process, paraffin oil (BDH, England) was introduced to the microchannel connected to the protein microchambers, isolating the protein solution in the microchamber. Finally, the mixing valves were turned on by pulling the connected plastic syringe. And the resulting mixed solutions were incubated under the paraffin oil. The crystals of the proteins were examined by using a polarized light microscope (Leica MZ 16, Germany) equipped with a CCD camera (SPOT Insight, Diagnostic Instruments).

4.3 Results and Discussions

4.3.1 Screening of protein crystallization conditions

A sparse matrix screening was performed by using the present microfluidic platform. In this method, the screening kit contains unique conditions with combinations of salts, precipitants, and buffers. Results from an initial screen can

produce crystals or solubility information, which allows optimization or development of rational strategies for subsequent screens.

To conduct a sparse matrix screening, we need to solve the following several issues: (i) the loading of protein and precipitant solutions into an array of microchambers; (ii) the mixing of protein and precipitants in parallel; (iii) the concentration control. Detail discussion about these issues will be shown in the following sections (**Figure 4.5**).

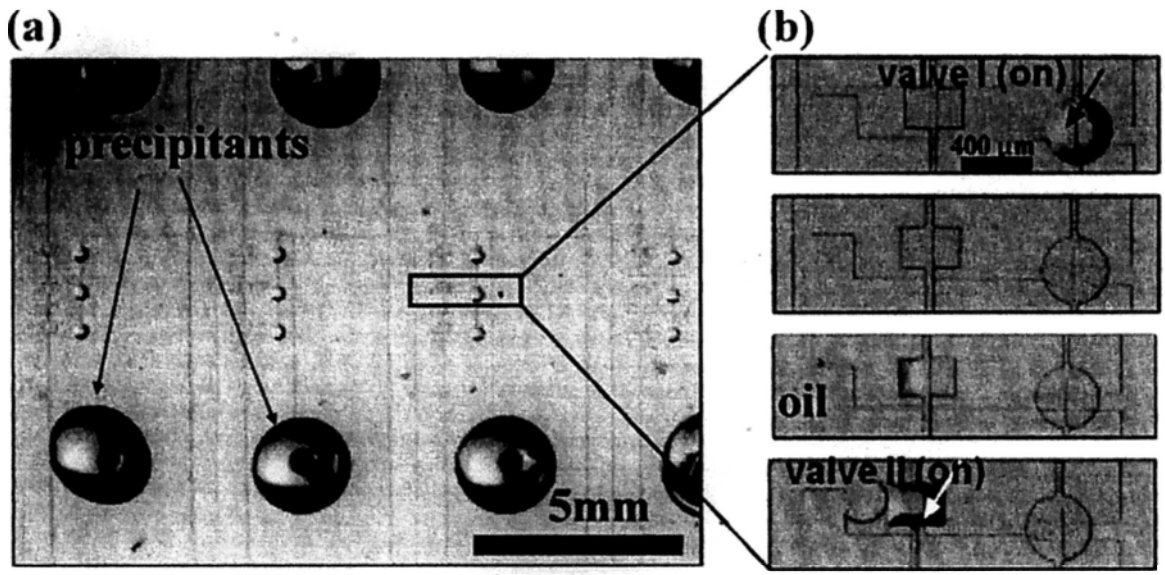

Figure 4.5. Liquid dispensing and mixing for screening of thaumatin crystallization conditions. (a) 48 precipitants and thaumatin solution were loaded to the inlets. (b) Series of images showing the dispensing and mixing processes.

4.3.2 The loading of protein and precipitants

The loading of protein and various precipitants into the nanoliter scale microchamber is usually difficult due to different properties of the fluids, such as viscosity and wettability. Recently several microfluidic systems for protein crystallization have been developed, such as FID, [10] SlipChip [57-59] and PhaseChip, [34]

which involve the liquid delivery into arrays of microchamber. Although the these microfluidic systems can lower the sample consumption and increase the throughput of the screening of protein crystallization, they still suffer from several issues. For instance, the FID method requires an extra pressure to delivery liquid into the microchamber.[10] And the SlipChip method needs to modify the glass surface and carefully control the movement of the glass chip.[57-59] The PhaseChip method requires enough microfluidic background and calculation to delivery droplet into the microchamber through microchannel. [34] These issues creates barrier for the end-user to adopt microfluidic systems to carrying out protein crystallization.

To solve these issues, we have already developed a degassed PDMS pumping method for delivering liquids at the nanoliter scales.[56] This method makes use of gas permeability of PDMS, in which the air concentration can be depleted in a vacuum chamber (10 kPa). The degassed PDMS can serve as an internal vacuum pumping source. When a liquid is deposited at the inlet of the degassed PDMS microchannel, the air flow to the microchannel will be blocked. As the continuous dissolving of air into the PDMS inside the sealed microchamber, a negative pressure will be generated, which served as pumping source to aspirate the liquid into the microchannel until all the empty place was filled.

In the present design, the introduction of PDMS membrane valve into the degassed PDMS pumping system allows us further controlling the dispensing of

liquid into a well defined dead-end microchamber as well as the isolating of the liquid after the dispensing. When a vacuum generated by a plastic syringe is applied in the control channel, the dispensing valves are turned on and the dead-end precipitant microchamber will be connected with the dispensing microchannel, the pre-stored vacuum power inside the dead-end PDMS microchamber will serve as the pumping source to aspirate the liquid into the dead-end microchamber. After the dispensing, the dispensing valve is turned off, by which the PDMS membrane valve blocks the dispensing channel and the microchamber. This finding indicates that we can temporally store the vacuum in a dead-end microchamber to control the liquid dispensing. What's more, due to the nature of this dispensing method by the degassed PDMS—the entire connected empty place will be filled by the liquid, we did not observed any air bubble or clotting in the dispensing of various precipitants and protein solutions.

4.3.2 The mixing of protein and precipitants

The control of mixing of solutions at the nanoliter scale is a challenge. Pneumatic valve has been adopted in the FID method to control the mixing time of protein and precipitants, however, in this method, the fluid channel is very small, usually a few tens of micrometer by which the protein and precipitant cannot be mixed fast. In our design, the mixing valve is 250 μm in width, 300 μm in length and 100 μm in height. This much larger mixing valve is designed to shorter the mixing time of the protein and precipitants.

To demonstrate the mixing of solutions controlled by the mixing valve, we filled the protein and precipitant microchamber with $Fe(NO_3)_3$ (0.25 M in 15% PEG6K) and KSCN (0.25 M in 15% PEG6K) aqueous solutions, respectively. As the mixing valve was turned on, a red line was observed at the interconnection area. The red area kept developing and finally reached a homogenous red solution (**Figure 4.6**).

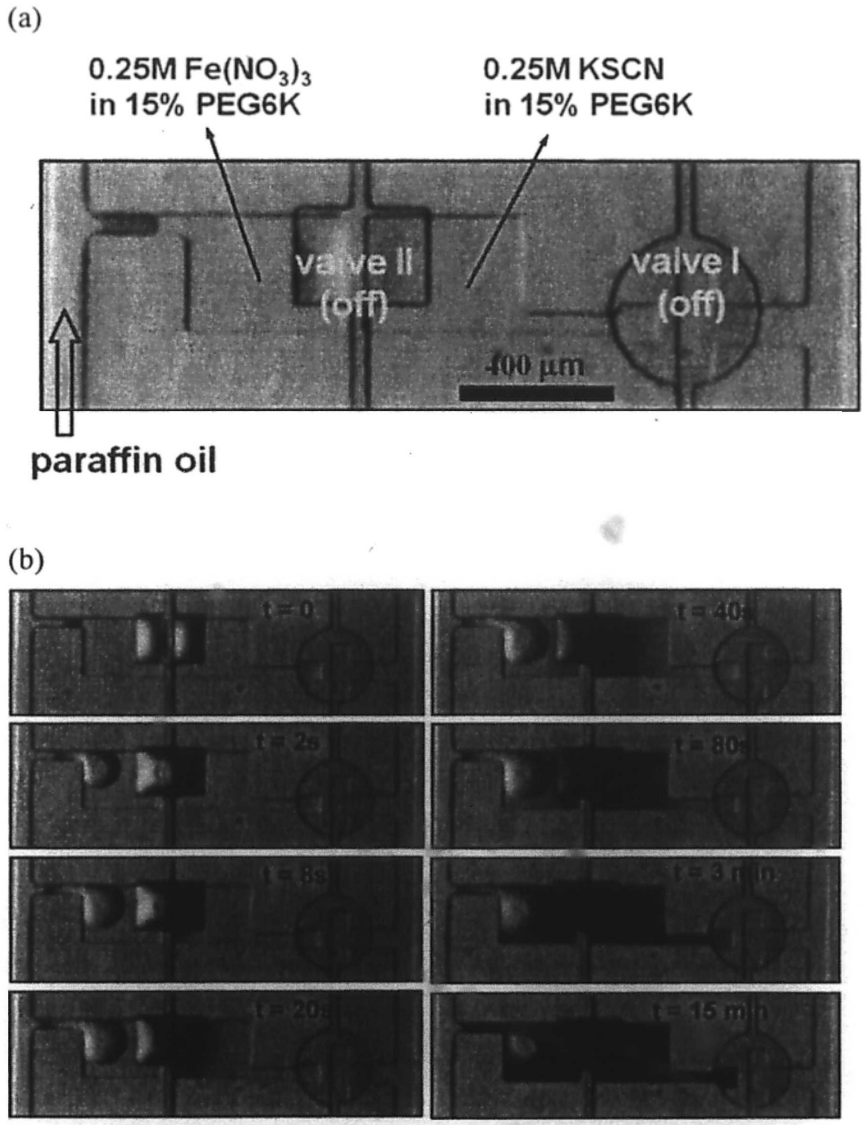

Figure 4.6 The mixing of $Fe(NO_3)_3$ (0.25 M in 15% PEG6K) and KSCN (0.25 M in 15% PEG6K) aqueous solutions controlled by the mixing valve. (a) Loading of aqueous solution into the reaction microchamber, where mixing did not occurred. (b) Time-lapse images showing the mixing process, where the mixing was triggered by the mixing valve. The red color indicated the mixing occurred.

In a real screening experiment, 144 trials were carried out simultaneously. In our design, all the mixing valves were connected and were controlled by a plastic syringe. After the dispensing of protein and precipitants into the microchambers, the mixing was triggered by pulling the syringe. The operation of the mixing valve is very simple and user friendly.

4.3.3 The concentration control

Varying the concentration of solutions at the nanoliter scale is a challenge due to the ultra small scale of the reagents. PhaseChip demonstrated the capability of controlling the concentration of aqueous solution by introducing some reservoir channel.[34] However, the PhaseChip method did not use the precipitant as the reservoir solutions, usually in a protein crystallization experiment, the precipitant is used as the reservoir to cause the water evaporated from the crystallizing droplet into the reservoir. In our design, we introduced reservoirs which are just next to the crystallizing microchamber. Thanks to the use of dispensing valves, we are able to dispense the reservoir with precipitant during the dispensing process, in which microchannel connected to the reservoir can also use for dispensing the precipitant microchamber controlling by the dispensing valves (**Figure 4.5**). Our method solves the issue of how to dispensing individual reservoirs with their corresponding crystallization conditions. **Figure 4.7** shows a polarized micrograph of the thaumatin crystals grown in the microchamber in the presence of side reservoir for 20 hours. What's more, since the reservoirs are always connected to the inlets for the precipitants, we can further control the concentration of the reservoirs by switching

solution at the inlets to a different concentration. We envision that this approach may allow further control of the protein crystallization solution either by concentrating or diluting.

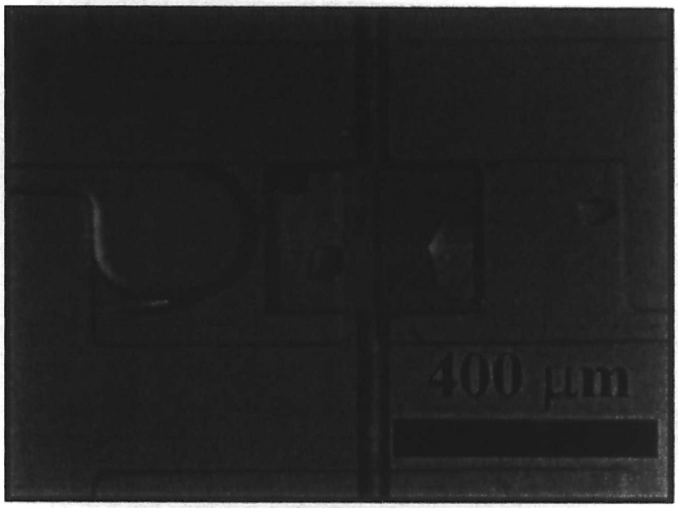

Figure 4.7. Polarized light micrograph of the thaumatin crystals grown in the crystallization microchamber for 20 hours. Thaumatin: 50 mg/ml in 0.1 M N-(2-acetamido)iminodiacetic acid buffer, pH 6.5; precipitant: 0.8 M potassium sodium tartrate tetrahydrate / 0.1 M HEPES buffer, pH 7.5.

4.4 Conclusion

A degassed PDMS microfluidic platform for screening of protein crystallization conditions was developed. This microfluidic platform combined degassed PDMS pumping method with PDMS membrane valve. The introduction of valves provides more functions of this pumping method, which allow us further controlling the dispensing, mixing and concentration control. We demonstrated the liquid dispensing and mixing of solutions in the microfluidic platform. A PDMS microchip with 144 trials was used to perform the screening of thaumatin crystallization conditions with commercial crystal screening kit. Without using any expensive dispensing system or equipment, we were able to dispense a large number of microchambers with protein

and precipitant as well as the reservoirs. We believe that this microfluidic platform may have great potential in the screening of protein crystallization conditions.

References

(1) Whitesides, G. M. *Nature* **2006**, *442*, 368.

(2) Manz, A.; Graber, N.; Widmer, H. M. *Sens. Actuator B-Chem.* **1990**, *1*, 244.

(3) Harrison, D. J.; Fluri, K.; Seiler, K.; Fan, Z. H.; Effenhauser, C. S.; Manz, A. *Science* **1993**, *261*, 895.

(4) Effenhauser, C. S.; Manz, A.; Widmer, H. M. *Anal. Chem.* **1993**, *65*, 2637.

(5) Effenhauser, C. S.; Paulus, A.; Manz, A.; Widmer, H. M. *Anal. Chem.* **1994**, *66*, 2949.

(6) Xia, Y. N.; Whitesides, G. M. *Annu. Rev. Mater. Sci.* **1998**, *28*, 153.

(7) Unger, M. A.; Chou, H. P.; Thorsen, T.; Scherer, A.; Quake, S. R. *Science* **2000**, *288*, 113.

(8) Rondelez, Y.; Tresset, G.; Tabata, K. V.; Arata, H.; Fujita, H.; Takeuchi, S.; Noji, H. *Nat. Biotechnol.* **2005**, *23*, 361.

(9) Lipman, E. A.; Schuler, B.; Bakajin, O.; Eaton, W. A. *Science* **2003**, *301*, 1233.

(10)Hansen, C. L.; Skordalakes, E.; Berger, J. M.; Quake, S. R. *Proc. Natl. Acad. Sci. U. S. A.* **2002**, *99*, 16531.

(11)Zheng, B.; Roach, L. S.; Ismagilov, R. F. *J. Am. Chem. Soc.* **2003**, *125*, 11170.

(12)Foquet, M.; Korlach, J.; Zipfel, W.; Webb, W. W.; Craighead, H. G. *Anal. Chem.* **2002**, *74*, 1415.

(13)Chan, E. Y.; Goncalves, N. M.; Haeusler, R. A.; Hatch, A. J.; Larson, J. W.; Maletta, A. M.; Yantz, G. R.; Carstea, E. D.; Fuchs, M.; Wong, G. G.; Gullans, S. R.; Gilmanshin, R. *Genome Res.* **2004**, *14*, 1137.

(14)Riehn, R.; Lu, M. C.; Wang, Y. M.; Lim, S. F.; Cox, E. C.; Austin, R. H. *Proc. Natl. Acad. Sci. U. S. A.* **2005**, *102*, 10012.

(15)Wang, Y. M.; Tegenfeldt, J. O.; Reisner, W.; Riehn, R.; Guan, X. J.; Guo, L.; Golding, I.; Cox, E. C.; Sturm, J.; Austin, R. H. *Proc. Natl. Acad. Sci. U. S. A.* **2005**, *102*, 9796.

(16)Squires, T. M.; Quake, S. R. *Rev. Mod. Phys.* **2005**, *77*, 977.

(17) Weibel, D. B.; DiLuzio, W. R.; Whitesides, G. M. *Nat. Rev. Microbiol.* **2007**, *5*, 209.

(18) deMello, A. J. *Nature* **2006**, *442*, 394.

(19) Scarpa, J. S.; Mueller, D. D.; Klotz, I. M. *J. Am. Chem. Soc.* **1967**, *89*, 6024.

(20) Ohta, H.; Ando, I.; Fujishige, S.; Kubota, K. *J. Polym. Sci. Pt. B-Polym. Phys.* **1991**, *29*, 963.

(21) Kubota, K.; Fujishige, S.; Ando, I. *Polym. J.* **1990**, *22*, 15.

(22) Yang, H.; Yan, X. H.; Cheng, R. S. *J. Polym. Sci. Pt. B-Polym. Phys.* **2000**, *38*, 1188.

(23) Winnik, F. M. *Macromolecules* **1990**, *23*, 233.

(24) Boutris, C.; Chatzi, E. G.; Kiparissides, C. *Polymer* **1997**, *38*, 2567.

(25) Wu, C.; Zhou, S. Q. *Macromolecules* **1995**, *28*, 8381.

(26) Schild, H. G.; Tirrell, D. A. *J. Phys. Chem.* **1990**, *94*, 4352.

(27) Fujishige, S.; Kubota, K.; Ando, I. *J. Phys. Chem.* **1989**, *93*, 3311.

(28) Tong, Z.; Zeng, F.; Zheng, X.; Sato, T. *Macromolecules* **1999**, *32*, 4488.

(29) Van Durme, K.; Van Assche, G.; Van Mele, B. *Macromolecules* **2004**, *37*, 9596.

(30) Furyk, S.; Zhang, Y.; Ortiz-Acosta, D.; Cremer, P. S.; Bergbreiter, D. E. *J. Polym. Sci. Part A: Polym. Chem.* **2006**, *44*, 1492.

(31) Mao, H. B.; Li, C. M.; Zhang, Y. J.; Bergbreiter, D. E.; Cremer, P. S. *J. Am. Chem. Soc.* **2003**, *125*, 2850.

(32) Leng, J.; Lonetti, B.; Tabeling, P.; Joanicot, M.; Ajdari, A. *Phys. Rev. Lett.* **2006**, *96*.

(33) Lau, B. T. C.; Baitz, C. A.; Dong, X. P.; Hansen, C. L. *J. Am. Chem. Soc.* **2007**, *129*, 454.

(34) Shim, J. U.; Cristobal, G.; Link, D. R.; Thorsen, T.; Jia, Y. W.; Piattelli, K.; Fraden, S. *J. Am. Chem. Soc.* **2007**, *129*, 8825.

(35) Mao, H.; Li, C.; Zhang, Y.; Furyk, S.; Cremer, P. S.; Bergbreiter, D. E. *Macromolecules* **2004**, *37*, 1031.

(36) Randall, G. C.; Doyle, P. S. *Proc. Natl. Acad. Sci. U. S. A.* **2005**, *102*, 10813.

(37) Chayen, N. E. *Trends in Biotechnology* **2002**, *20*, 98.

(38) Yee, A.; Pardee, K.; Christendat, D.; Savchenko, A.; Edwards, A. M.; Arrowsmith, C. H. *Accounts Chem. Res.* **2003**, *36*, 183.

(39) Skolnick, J.; Fetrow, J. S.; Kolinski, A. *Nat. Biotechnol.* **2000**, *18*, 283.

(40) Brenner, S. E. *Nat. Rev. Genet.* **2001**, *2*, 801.

(41) Blundell, T. L.; Jhoti, H.; Abell, C. *Nat. Rev. Drug Discov.* **2002**, *1*, 45.

(42) Stevens, R. C.; Yokoyama, S.; Wilson, I. A. *Science* **2001**, *294*, 89.

(43) Stevens, R. C. *Struct. Fold. Des.* **2000**, *8*, R177.

(44) Abola, E.; Kuhn, P.; Earnest, T.; Stevens, R. C. *Nat. Struct. Biol.* **2000**, *7*, 973.

(45) Sanchez, R.; Pieper, U.; Melo, F.; Eswar, N.; Marti-Renom, M. A.; Madhusudhan, M. S.; Mirkovic, N.; Sali, A. *Nat. Struct. Biol.* **2000**, *7*, 986.

(46) McPherson, A. *Crystallization of Biological Macromolecules*; Cold Spring Harbor Laboratory Press: Cold Spring Harbor, 1999.

(47) Luft, J. R.; Collins, R. J.; Fehrman, N. A.; Lauricella, A. M.; Veatch, C. K.; DeTitta, G. T. *J. Struct. Biol.* **2003**, *142*, 170.

(48) Walter, T. S.; Diprose, J.; Brown, J.; Pickford, M.; Owens, R. J.; Stuart, D. I.; Harlos, K. *J. Appl. Crystallogr.* **2003**, *36*, 308.

(49) Kuhn, P.; Wilson, K.; Patch, M. G.; Stevens, R. C. *Curr. Opin. Chem. Biol.* **2002**, *6*, 704.

(50) Zheng, B.; Tice, J. D.; Roach, L. S.; Ismagilov, R. F. *Angew. Chem.-Int. Edit.* **2004**, *43*, 2508.

(51) Li, L.; Mustafi, D.; Fu, Q.; Tereshko, V.; Chen, D. L.; Tice, J. D.; Ismagilov, R. F. *Proc. Natl. Acad. Sci. U. S. A.* **2006**, *103*, 19243.

(52) Mukhopadhyay, R. *Anal. Chem.* **2007**, *79*, 3248.

(53) Chayen, N. E.; Stewart, P. D. S.; Blow, D. M. *J. Cryst. Growth* **1992**, *122*, 176.

(54) Darcy, A.; Elmore, C.; Stihle, M.; Johnston, J. E. *J. Cryst. Growth* **1996**, *168*, 175.

(55) Darcy, A.; Mac Sweeney, A.; Stihle, M.; Haber, A. *Acta Crystallogr. Sect. D-Biol. Crystallogr.* **2003**, *59*, 396.

(56) Zhou, X.; Lau, L.; Lam, W. W. L.; Au, S. W. N.; Zheng, B. *Anal. Chem.* **2007**, *79*, 4924.

(57) Li, L.; Du, W. B.; Ismagilov, R. F. *J. Am. Chem. Soc.* **2010**, *132*, 112.

(58) Li, L.; Du, W. B.; Ismagilov, R. *J. Am. Chem. Soc.* **2010**, *132*, 106.

(59) Du, W. B.; Li, L.; Nichols, K. P.; Ismagilov, R. F. *Lab Chip* **2009**, *9*, 2286.

(60) Lee, J. N.; Park, C.; Whitesides, G. M. *Anal. Chem.* **2003**, *75*, 6544.

(61) Zheng, B.; Tice, J. D.; Ismagilov, R. F. *Anal. Chem.* **2004**, *76*, 4977.

(62) Song, H.; Chen, D. L.; Ismagilov, R. F. *Angew. Chem.-Int. Edit.* **2006**, *45*, 7336.

(63) Hosokawa, K.; Sato, K.; Ichikawa, N.; Maeda, M. *Lab Chip* **2004**, *4*, 181.

(64) Eddings, M. A.; Gale, B. K. *J. Micromech. Microeng.* **2006**, *16*, 2396.

(65) Fosser, K. A.; Nuzzo, R. G. *Anal. Chem.* **2003**, *75*, 5775.

(66) Monahan, J.; Gewirth, A. A.; Nuzzo, R. G. *Anal. Chem.* **2001**, *73*, 3193.

(67) Duffy, D. C.; McDonald, J. C.; Schueller, O. J. A.; Whitesides, G. M. *Anal. Chem.* **1998**, *70*, 4974.

(68) Merkel, T. C.; Bondar, V. I.; Nagai, K.; Freeman, B. D.; Pinnau, I. *J. Polym. Sci. Pt. B-Polym. Phys.* **2000**, *38*, 415.

(69) Watson, J. M.; Baron, M. G. *J. Membr. Sci.* **1995**, *106*, 259.

(70) Afroze, F.; Nies, E.; Berghmans, H. *J. Mol. Struct.* **2000**, *554*, 55.

(71) Mei, Q.; Fredrickson, C. K.; Lian, W.; Jin, S. G.; Fan, Z. H. *Anal. Chem.* **2006**, *78*, 7659.

(72) Winnik, F. M. *Polymer* **1990**, *31*, 2125.

(73) Rolland, J. P.; Van Dam, R. M.; Schorzman, D. A.; Quake, S. R.; DeSimone, J. M. *J. Am. Chem. Soc.* **2004**, *126*, 2322.

(74) Huang, Y. Y.; Castrataro, P.; Lee, C. C.; Quake, S. R. *Lab Chip* **2007**, *7*, 24.

(75) Zheng, B.; Ismagilov, R. F. *Angew. Chem.-Int. Edit.* **2005**, *44*, 2520.